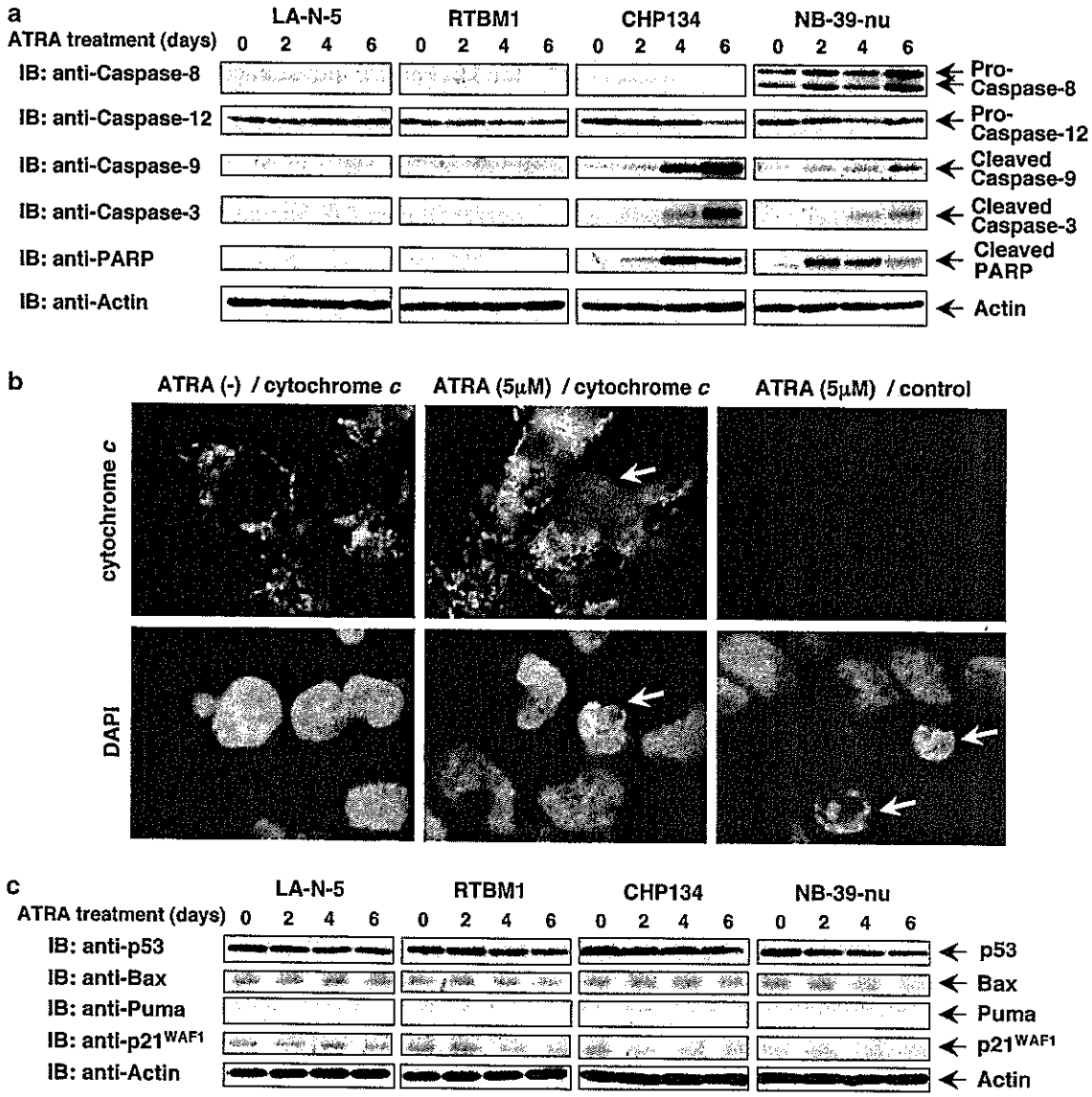

Figure 2 Caspase-9 and caspase-3 are cleaved during the all-*trans* retinoic acid (ATRA)-mediated apoptosis in CHP134 and NB-39-nu cells. (a) Immunoblot analysis for various caspases and poly-ADP-ribose polymerase (PARP) in response to ATRA. The indicated neuroblastoma cell lines were treated with 5 μM of ATRA or left untreated. At the indicated time points after the treatment with ATRA, whole-cell lysates were prepared, and analysed by immunoblotting with indicated antibodies. Actin expression was used as a loading control (bottom). (b) ATRA-induced cytoplasmic release of cytochrome *c* in CHP134 cells. CHP134 cells were seeded onto coverslips, and cultured in the presence or absence of 5 μM of ATRA. Four days after the treatment with ATRA, cells were fixed and stained with a monoclonal antibody against cytochrome *c* (top, left and middle) or with a normal mouse IgG (top, right). The cell nuclei were stained with 4,6-diamidino-2-phenylindole (DAPI) (bottom). The arrows indicate apoptotic cells with condensed and fragmented nuclei. (c) Expression levels of p53 and its direct target gene products in response to ATRA. At the indicated time periods after the treatment with ATRA, whole-cell lysates were prepared, and subjected to immunoblotting with antibodies against p53, Bax, Puma, $p21^{WAF1}$ and actin. Immunoblotting for actin is shown as a control for protein loading (bottom).

Figure 1 Effects of all-*trans* retinoic acid (ATRA) on cell proliferation of LA-N-5, RTBM1, CHP134 and NB-39-nu neuroblastoma-derived cell lines. (a) Growth curves of the indicated neuroblastoma cell lines in the presence or absence of ATRA. Cells were grown in the standard culture medium, and treated with 5 μM of ATRA. At the indicated time points after the treatment with ATRA, cells were trypsinized, harvested and number of viable cells was counted in triplicate. (b) ATRA-induced morphological changes of neuroblastoma cell lines. Cells were exposed to ATRA at a final concentration of 5 μM or left untreated. Six days after the treatment with ATRA, cells were examined by phase-contrast microscopy. (c and d) ATRA-induced cell death through apoptosis in CHP134 and NB-39-nu cells. Cells were treated with the indicated concentrations of ATRA or left untreated, and incubated for up to 6 days. At the indicated time points after the treatment with ATRA, cells were collected, fixed and stained with propidium iodide (PI). The DNA content of the cells was then examined by flow cytometry (c). The number of cells with sub-G1 DNA content was counted in triplicate (d).

that cytochrome *c* release from mitochondria might play an important role in ATRA-induced apoptotic cell death in neuroblastoma cells.

As the neuroblastoma cell lines that we examined carry wild-type p53 (data not shown), we investigated whether p53 could contribute to the ATRA-mediated apoptotic cell death. For this purpose, whole-cell lysates prepared from the indicated neuroblastoma cells exposed to 5 μM of ATRA for 0, 2, 4 and 6 days were processed for immunoblotting with the indicated antibodies. As shown in Figure 2c, the amounts of p53 remained unchanged or slightly decreased after ATRA treatment. In accordance with these results, ATRA had undetectable effects on the expression levels of p53-responsible Bax, Puma and $p21^{WAF1}$, which are implicated in the p53-dependent apoptosis and/or cell cycle arrest (Culmsee and Mattson, 2005). In addition, ATRA failed to induce the phosphorylation of p53 at Ser-15 (data not shown). Thus, it is likely that ATRA-mediated apoptotic cell death in neuroblastoma cells may be regulated in a p53-independent manner.

Differential expression of antiapoptotic Bcl-2 in neuroblastoma cells

To investigate the regulatory mechanisms of apoptotic response to ATRA in neuroblastoma cells, we examined the expression levels of Bcl-2 family proteins, which directly control the mitochondrial pathway of apoptosis. It is worth noting that antiapoptotic Bcl-2 was constitutively expressed at high levels in LA-N-5 as well as RTBM1 cells, whereas CHP134 and NB-39-nu cells expressed Bcl-2 at extremely low levels (Figure 3a). Antiapoptotic Bcl-x_L was expressed at low levels in all cell lines examined. In accordance with the previous observations showing that proapoptotic Bim and Bmf are highly expressed in neuronal cells (Puthalakath *et al*., 2001; Okuno *et al*., 2004; Shi *et al*., 2004), Bim and Bmf were expressed at high levels in all of the cell lines that we examined, but their expression levels remained unchanged in the presence of ATRA.

To determine whether Bcl-2 could contribute to the acquisition of the ATRA-resistant phenotype of neuroblastoma cells, CHP134 cells were transfected with the expression plasmid for Bcl-2 or with the empty plasmid, and their sensitivity to ATRA was examined by flow cytometry. As shown in Figure 3b, Bcl-2 was successfully overexpressed in CHP134 cells as examined by immunoblotting. Interestingly, enforced expression of Bcl-2 inhibited the ATRA-mediated proteolytic cleavage of caspase-3. Consistent with these results, flow cytometric analysis demonstrated that ectopic expression of Bcl-2 significantly reduced the number of cells with sub-G1 DNA content induced by ATRA treatment (Figure 3c and d), suggesting that Bcl-2 might play a critical role in the regulation of apoptotic cell death in neuroblastoma cells.

To further confirm this possibility, we examined the effects of the Bcl-2 inhibitor HA14-1 (Wang *et al*., 2000) on the ATRA-mediated apoptotic response of neuroblastoma cells. RTBM1 cells were treated with 5 μM of ATRA or left untreated for 6 days, and then incubated in the presence or absence of HA14-1 (15, 30 or 50 μM) for 3 h. Phase-contrast microscopic analysis showed that the incubation with ATRA followed by HA14-1 treatment significantly enhanced the apoptotic response of RTBM1 cells, whereas HA14-1 treatment alone increased the number of apoptotic cells to a lesser degree (Figure 4a). Similar results were also obtained by flow cytometric analysis (Figure 4b and c). To examine whether the ATRA-mediated apoptosis in RTBM1 cells induced by HA14-1 treatment could be associated with the activation of the mitochondria-dependent apoptotic pathway, we performed immunoblot analysis. As shown in Figure 4d, HA14-1 treatment at 30 μM or less did not promote the activation of caspase-9 and caspase-3, whereas a small amount of the cleaved caspase-9 and caspase-3 were detectable in RTBM1 cells exposed to 50 μM of HA14-1 alone. Intriguingly, pre-treatment of RTBM1 cells with ATRA enhanced the proteolytic cleavage of caspase-9 and caspase-3 induced by HA14-1 at a final concentration of 50 μM.

To ask whether Bcl-2 could play an important role in ATRA-mediated apoptotic response in primary neuroblastomas, 10 sporadically found neuroblastomas were subjected to both primary culture and reverse transcriptase–polymerase chain reaction (RT-PCR) analysis for *bcl-2*. In five cases, ATRA treatment induced strong outgrowth of neurites as compared with control culture (Figure 5a, left). In the other three cases, ATRA had undetectable effects (data not shown). It is worth noting that many cells underwent cell death after ATRA treatment in the remaining two cases (Figure 5a, right). We also examined the expression levels of *bcl-2* of these 10 primary neuroblastoma samples and four neuroblastoma-derived cell lines by RT–PCR. LA-N-5 and RTBM1 cells abundantly expressed *bcl-2*, whereas CHP134 and NB-39-nu did not (Figure 5b), which was consistent with immunoblotting as shown in Figure 3a. Of particular interest, RT–PCR analysis revealed that two primary cases that underwent cell death in response to ATRA (N-9 and N-10) expressed *bcl-2* at undetectable levels (Figure 5c). In a sharp contrast, the expression of *bcl-2* was detected in the remaining cases, except N-3. Taken together, our present results strongly suggest that Bcl-2 is a key regulator for ATRA-mediated apoptotic cell death in neuroblastoma cells.

Discussion

Retinoic acid is one of the potent antitumor agents that has been used successfully to treat certain human tumors including neuroblastomas (Freemantle *et al*., 2003). Indeed, neuroblastoma patients treated with RA have increased survival rate without severe side effects (Villablanca *et al*., 1995; Matthay *et al*., 1999). Accumulating evidences suggest that RA plays an important role in the regulation of neuroblastoma apoptosis as well as differentiation (Melino *et al*.,

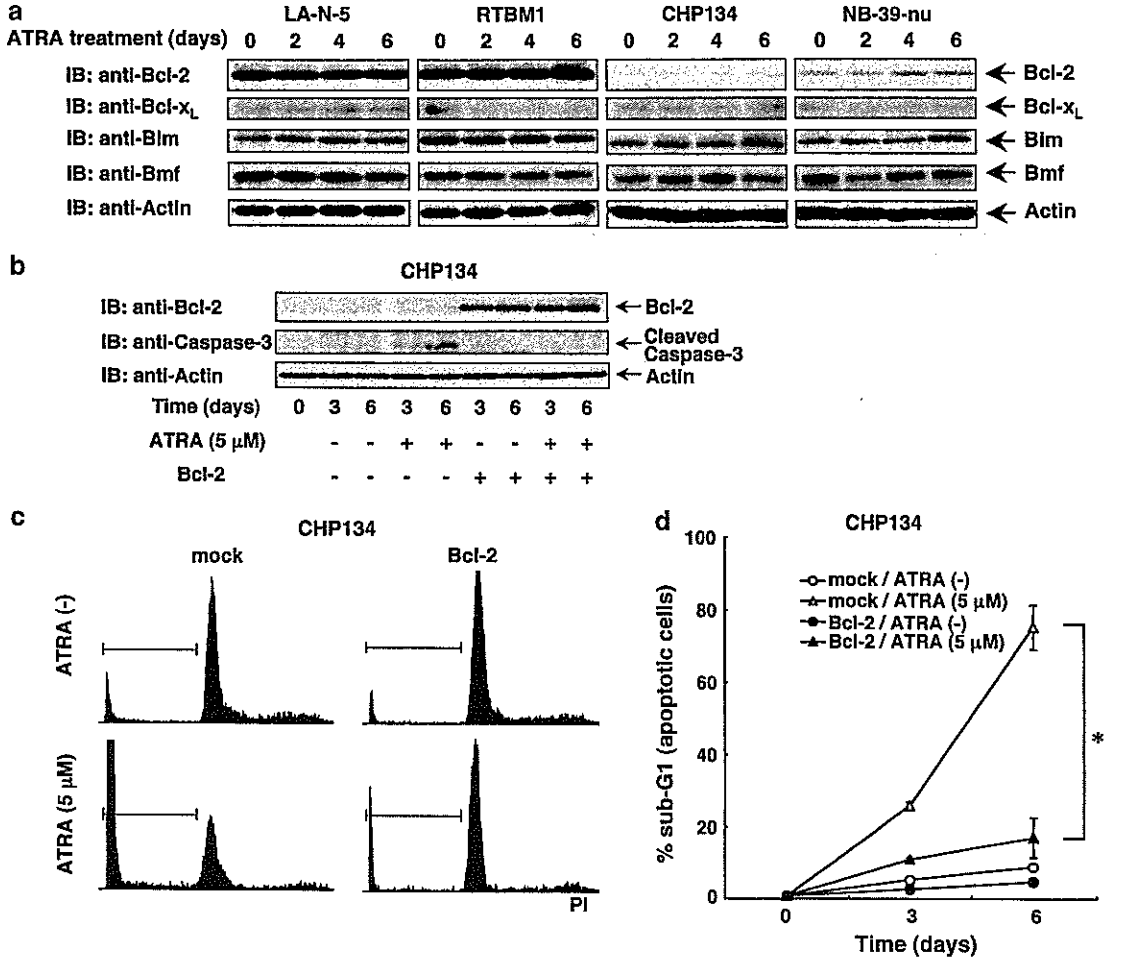

Figure 3 Differential expression of antiapoptotic Bcl-2 protein. (a) The indicated neuroblastoma cell lines were cultured in standard culture medium containing all-*trans* retinoic acid (ATRA) at a final concentration of 5 μM. At the indicated time points after the treatment with ATRA, whole-cell lysates were prepared, and analysed by immunoblotting with the antibodies against the indicated Bcl-2 family proteins. Actin expression was examined as a loading control (bottom). (b) Overexpression of Bcl-2. CHP134 cells were transiently transfected with the expression plasmid for Bcl-2 or with the empty plasmid. Twelve hours after the transfection, cells were treated with or without 5 μM ATRA, and incubated for additional 3 or 6 days. Whole-cell lysates were prepared, and the expression levels of Bcl-2 (top) and the amounts of the cleaved caspase-3 (middle) were examined by immunoblotting. Actin is shown as a control for protein loading (bottom). (c and d) Flow cytometry. CHP134 cells were transiently transfected as described in (b). At the indicated time periods after the treatment with ATRA, cells were collected, fixed and stained with PI. The DNA content of the cells was examined by flow cytometry. Representative results on day 6 are shown in (c). The number of cells with sub-G1 DNA content was counted in triplicate (d). $*P<0.01$.

1997; van Noesel and Versteeg, 2004). However, certain neuroblastomas display an RA-resistant phenotype (Reynolds and Lemons, 2001). To further improve the therapeutic effects of RA on neuroblastomas, it is necessary to clarify the detailed molecular mechanisms underlying the RA-mediated neuroblastoma differentiation and/or apoptosis. In the present study, we have found that ATRA causes growth suppression and subsequent neuronal differentiation in human neuroblastoma-derived LA-N-5, RTBM1, CHP134 and NB-39-nu cells to various degrees. Among them, CHP134 and NB-39-nu cells, which express antiapoptotic Bcl-2 at extremely low levels, underwent p53-independent apoptotic cell death in response to ATRA. In contrast, LA-N-5 and RTBM1 cells abundantly expressed Bcl-2, and we did not detect apoptotic cell death upon ATRA treatment. Enforced expression of Bcl-2 in CHP134 cells inhibited the ATRA-mediated apoptosis, and HA14-1-mediated inhibition of the endogenous Bcl-2 in RTBM1 cells enhanced the ATRA-dependent apoptotic cell death. Moreover, studies using primary neuroblastoma tissues showed that ATRA had toxic effect on two out of 10 primary cultures, and these ATRA-sensitive tumors did not express *bcl-2*. Thus, it is likely that antiapoptotic Bcl-2 plays a crucial role in the regulation of the ATRA-mediated apoptotic response in neuroblastomas.

Our present study revealed that neuroblastoma cells can be divided into two groups with respect to the ATRA-induced apoptotic response. CHP134 and NB-39-nu cells underwent apoptotic cell death in response to ATRA, whereas LA-N-5 and RTBM1 cells did not. Consistent with the mitochondria-dependent intrinsic apoptotic pathway of caspase activation (Degterev

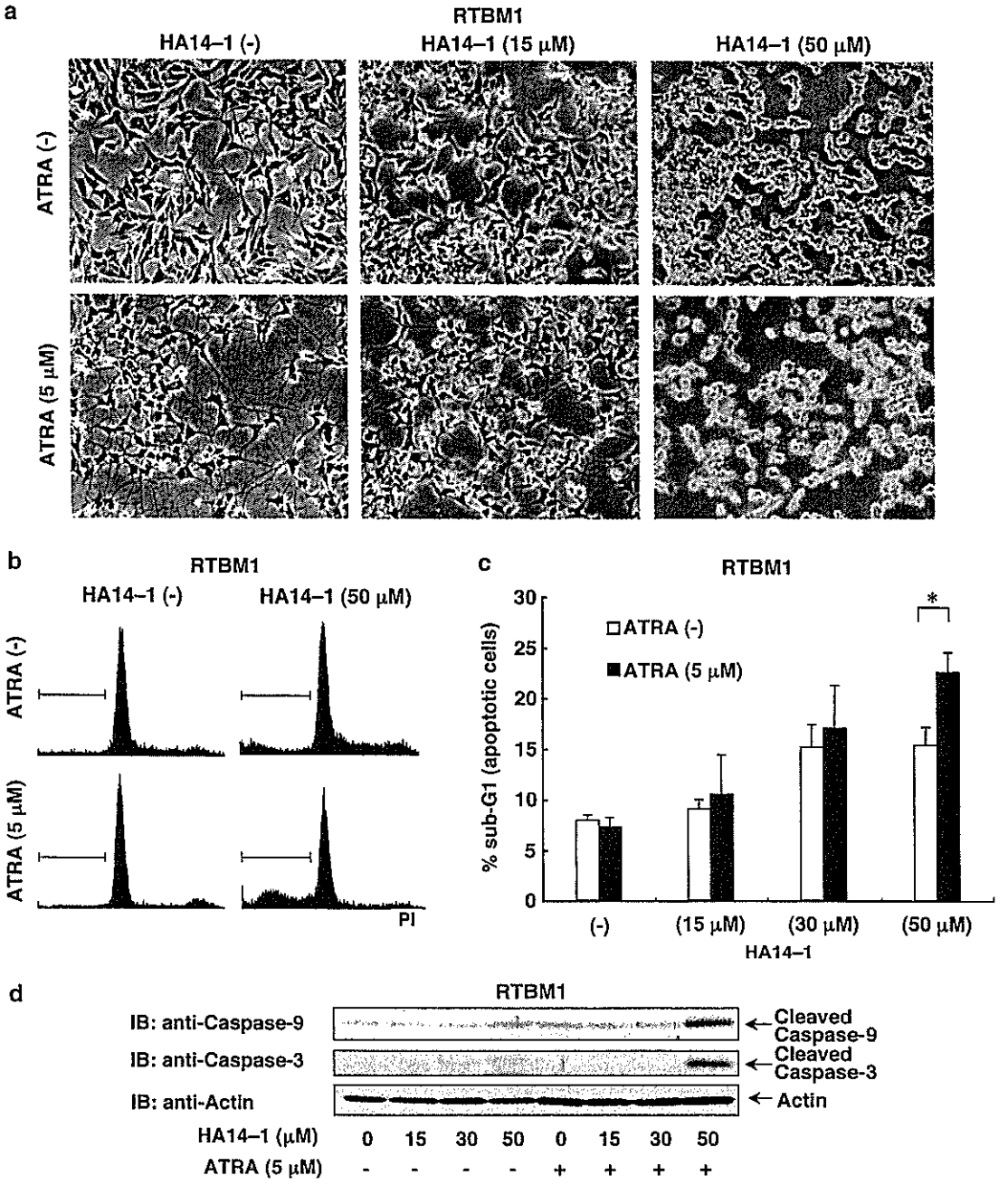

Figure 4 Bcl-2 inhibitor HA14-1 induces apoptosis of all-*trans* retinoic acid (ATRA)-treated RTBM1 cells. (a) Morphological changes after HA14-1 treatment of RTBM1 cells. RTBM1 cells were cultured with or without 5 μM ATRA for 6 days in advance, and then treated with HA14-1, a specific inhibitor of Bcl-2, at the indicated concentrations in standard medium for 3 h. Cells were examined by phase-contrast microscopy and photographed after the treatment. (b and c) FACS analysis. RTBM1 cells were treated with ATRA and HA14-1 as described in (a). Cells were collected, fixed and stained with PI. The DNA content of the cells was examined by flow cytometry and representative results are shown in (b). The number of cells with sub-G1 DNA content was counted in triplicate (c). *$P<0.05$. (d) Immunoblotting. Whole-cell lysates of RTBM1 treated with ATRA and HA14-1 were prepared to examine the amounts of cleaved caspase-9 and caspase-3. Actin is shown as a loading control.

et al., 2003), ATRA treatment in CHP134 cells caused a cytoplasmic release of the mitochondrial inter-membrane protein cytochrome *c*, and a sequential proteolytic cleavage of caspase-9, caspase-3 and its physiological substrate PARP. Similar results were obtained in NB-39-nu cells. Our previous observation also demonstrated that activation and nuclear translocation of caspases were associated with prognosis of primary neuroblastomas (Nakagawara *et al.*, 1997). Therefore, the molecular mechanism(s) of RA-induced activation of caspases in neuroblastoma cells needs to be clarified.

In response to a variety of apoptotic stimuli, p53 is induced to be stabilized and subsequently transactivates a number of proapoptotic genes that encode Bcl-2

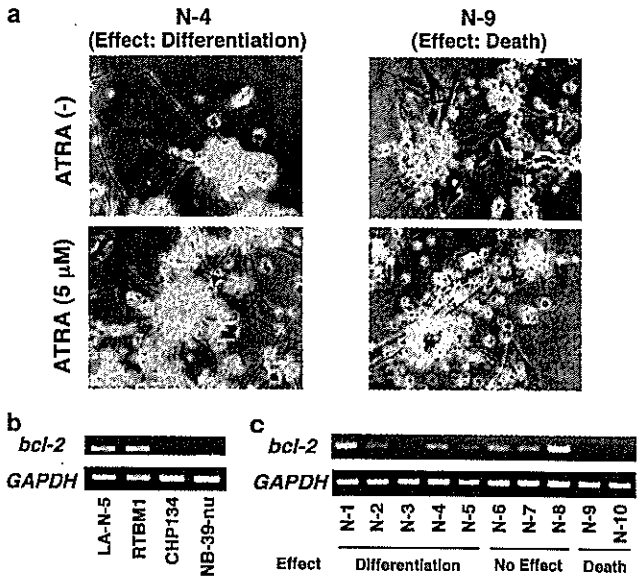

Figure 5 Primary culture and *bcl-2* expression of sporadic neuroblastomas. (a) Primary tumor cells prepared from 10 sporadically found neuroblastoma tissues were cultured with or without 5 μM of ATRA. After 4 days, cells were examined by phase-contrast microscope, and morphological changes of two representative cases are shown. (b and c) RT–PCR analysis. Total RNA was purified from the indicated neuroblastoma cell lines (b) and fresh-frozen tissues of primary neuroblastomas (c), and subjected to RT–PCR using specific primers for *bcl-2*. N-1 to N-10 indicates the case numbers, and the effects of ATRA on primary cultures are described at the bottom of this panel. Glyceraldehyde-3-phosphate dehydrogenase (*GAPDH*) expression is shown as an internal control.

family proteins including Bax (Culmsee and Mattson, 2005). It has been well documented that Bax acts on the mitochondria to induce mitochondrial permeability transition, and thereby regulating the cytoplasmic release of cytochrome *c* (Antonsson, 2001). Neuroblastoma cell lines that we examined in this study carry wild-type p53. Under our experimental conditions, however, we could not detect the ATRA-mediated upregulation of the endogenous p53 as well as Bax. Similarly, the p53-responsible $p21^{WAF1}$ and proapoptotic Puma were not accumulated in response to ATRA. As described (Nikolaev *et al*., 2003), p53 might not be functional in neuroblastoma cells due to its abnormal cytoplasmic retention. Consistent with this notion, p53 was predominantly expressed in the cytoplasm of neuroblastoma cells examined in this study (data not shown). We have previously shown that cytoplasmic p53 is translocated into the nucleus of CHP134 cells in response to ATRA (Takada *et al*., 2001); however, our present results suggest that translocated p53 was not functional. Indeed, it is reported that p53 in neuroblastoma cells is not functional even after its enforced translocation into the nucleus (Ostermeyer *et al*., 1996). Thus, it is likely that the ATRA-mediated apoptotic cell death in neuroblastoma cells is regulated in a p53-independent manner.

Among other regulators of mitochondrial pathway of apoptosis, Bcl-2 family proteins are critical determinants of mitochondrial membrane potential, which controls the cytoplasmic release of cytochrome *c* from mitochondria and thereby regulating apoptotic cell death (Cory *et al*., 2003). They are divided into two subfamilies based on their biological roles. Antiapoptotic subfamily includes Bcl-2 and Bcl-x_L and proapoptotic subfamily includes Bax, Bim and Bmf. The balance between these two groups determines the fate of cells. Antiapoptotic Bcl-2 is one of the most important members that inhibits the mitochondria-dependent apoptotic pathway triggered by diverse cytotoxic agents through blocking mitochondrial permeability transition. Indeed, the upregulation of Bcl-2 was associated with the drug-resistant phenotype of certain human tumors (Dole *et al*., 1994; Lombet *et al*., 2001). Most intriguingly, our expression studies revealed that antiapoptotic Bcl-2 was constitutively overexpressed in LA-N-5 and RTBM1 cells, whereas its expression levels were extremely low in CHP134 and NB-39-nu cells. In response to ATRA, Bcl-2 was slightly induced to be accumulated in NB-39-nu cells; however, it was maintained at extremely low levels in CHP134 cells. Furthermore, two primary neuroblastomas on which ATRA had toxic effect in primary culture did not express *bcl-2*, similar to CHP134 and NB-39-nu cells. Interestingly, ATRA induced differentiation in five cases and had undetectable effects on three cases, but cell death was induced in two cases. Considering that RA treatment contributed to survival of 17% of patients with aggressive neuroblastomas (Matthay *et al*., 1999), our present results using primary neuroblastomas seem to be reliable. Taken together, it is likely that ATRA potentially have toxic effect on certain neuroblastoma cells (both primary cells and cell lines) that express little Bcl-2. Our current results also revealed that enforced expression of Bcl-2 in CHP134 cells inhibited the ATRA-mediated apoptosis in association with the activation of caspase-3. Furthermore, ATRA treatment of RTBM1 cells followed by HA14-1 exposure underwent apoptotic cell death through mitochondrial pathway. These observations also support the importance of Bcl-2 in the regulation of apoptotic response of neuroblastoma cells to RA.

Although it is still unclear whether the expression levels of Bcl-2 could be correlated with the prognosis of neuroblastoma patients (Romani and Lu, 1994; Gallo *et al*., 2003; Abel *et al*., 2005), it is possible that Bcl-2 plays a key role at least in part in the regulation of ATRA-mediated apoptotic cell death in neuroblastoma cells. In this connection, the antisense RNA-mediated knockdown of the endogeneous Bcl-2 has been employed to treat certain tumors (Kim *et al*., 2004). Recently, a novel Bcl-2 inhibitor that has an antitumor effect on solid tumors has been developed (Oltersdorf *et al*., 2005). Based on our present findings, the combination of RA with Bcl-2-specific inhibitor might provide a novel therapeutic strategy for the treatment of neuroblastomas, instead of the classical chemotherapy that frequently has multi-organ side effects.

Materials and methods

Cell lines and transfection

Human neuroblastoma-derived cell lines, including LA-N-5, RTBM1, CHP134 and NB-39-nu, were maintained in RPMI 1640 medium supplemented with 10% heat-inactivated fetal bovine serum, penicillin (50 U/ml) and streptomycin (50 μg/ml) at 37°C in a humidified atmosphere of 5% CO_2 in the air. For transfection, CHP134 cells were transfected with the expression plasmid encoding human Bcl-2 or with the empty plasmid by electroporation using a Nucleofector (Amaxa Biosystems, Koeln, Germany) according to the manufacturer's protocol.

Reagents

All-*trans* retinoic acid was purchased from Sigma (St Louis, MO, USA) dissolved in dimethylsulfoxisde (DMSO) at a final concentration of 5 mM, and kept at −80°C. Bcl-2 inhibitor HA14-1 was purchased from Sigma, dissolved in DMSO as a 10 mM stock solution and stored at −20°C. All reagents were of the highest quality available.

Proliferation assay

LA-N-5 and RTBM1 cells were plated in triplicate at a density of 1×10^5 per well in 12-well culture plates. CHP134 and NB-39-nu cells were seeded in triplicate at a density of 1×10^4 in 12-well plates. Twelve hours after seeding the cells, cells were treated with ATRA at a final concentration of 5 μM or left untreated, and medium was replaced every 2 days. At the indicated time points after the treatment with ATRA, cells were trypsinized and number of viable cells was directly scored by using the hemocytometer.

Flow cytometric analysis

Cells were exposed to the indicated concentration of ATRA. At the indicated time points after the treatment with ATRA, cells were collected by brief centrifugation, and fixed with 70% ethanol at −20°C. The cells were washed with phosphate-buffered saline (PBS), resuspended in phosphate-citrate buffer (4 mM citric acid, 200 mM Na_2HPO_4) and kept at room temperature for 15 min. The cells were then centrifuged and resuspended in a solution containing 40 μg/ml of propidium iodide and 0.05% RNase A, and incubated in the dark for 30 min. Before performing flow cytometric analysis, cells were filtered through a 40-μm nylon mesh. DNA content was analysed by FACScan flow cytometer (Becton Dickinson, Oxford, UK).

Immunoblot analysis

Cells were washed twice with ice-cold PBS, lysed in a sodium dodecyl sulfate (SDS)-sample buffer containing 10% glycerol, 5% β-mercaptoethanol, 2.3% SDS and 62.5 mM Tris-HCl, pH 6.8, and then boiled for 3 min. The protein concentrations were determined using Bio-Rad protein assay dye reagent (Bio-Rad Laboratories, Hercules, CA, USA). Bovine serum albumin (BSA) was used as a standard. Aliquots (20 μg) of whole-cell lysates were separated by SDS–polyacrylamide gel electrophoresis and electrophoretically transferred onto polyvinylidene difluoride membranes (Immobilon-P, Millipore, Bedford, MA, USA). The membranes were blocked with 0.3% non-fat milk in Tris-buffered saline containing 0.1% Tween-20 and incubated with appropriate primary antibodies at room temperature for 1 h followed by incubation with the horseradish peroxidase-conjugated secondary antibodies (Cell Signaling Technology Inc., Beverly, MA, USA). Immunoreactive bands were visualized by using ECL system (Amersham Biosciences, Uppsala, Sweden). The primary antibodies used in this study were as follows: polyclonal anti-caspase-12 (Cell Signalling Technology Inc.), polyclonal anti-caspase-3 (Calbiochem, San Diego, CA, USA), polyclonal anti-PARP (Cell Signaling Technology Inc.), polyclonal anti-PUMA (ab9643; Abcam, Cambridge, UK), polyclonal anti-$p21^{WAF1}$ (H-164; Santa Cruz Biotechnology), polyclonal anti-Bim (Cell Signaling Technology Inc.), polyclonal anti-Bmf (Cell Signaling Technology Inc.), polyclonal anti-actin (20-33; Sigma), monoclonal anti-caspase-8 (5F7; Medical & Biological Laboratories, Nagoya, Japan), monoclonal anti-caspase-9 (5B4; Medical & Biological Laboratories), monoclonal anti-p53 (DO-1; Oncogene Research Products, Cambridge, MA, USA), monoclonal anti-Bax (6A7; eBioscience, San Diego, CA, USA), monoclonal anti-Bcl-2 (100; Santa Cruz Biotechnology); and monoclonal anti-Bcl-x_L (H-5; Santa Cruz Biotechnology) antibodies.

Immunofluorescent staining

CHP134 cells were grown on coverslips in standard culture medium in the presence or absence of 5 μM of ATRA for 4 days. Cells were washed with ice-cold PBS, fixed with 3.7% formaldehyde in PBS for 30 min, permeabilized with 0.2% Triton X-100 in PBS for 5 min and then blocked with 3% BSA in PBS for 1 h at room temperature. After blocking, cells were incubated with a monoclonal antibody against cytochrome *c* (6H2.B4; BD PharMingen, San Jose, CA, USA) or with a normal mouse IgG for 1 h at room temperature, followed by the incubation with fluorescein isothiocyanate-conjugated secondary antibody against mouse IgG (Santa Cruz Biotechnology). The cell nuclei were stained with DAPI. The coverslips were mounted onto glass slides, and the stained cells were examined by using a confocal laser scanning microscope (Olympus).

Primary culture

RPMI 1640 medium supplemented with 10% heat-inactivated fetal bovine serum, penicillin (50 U/ml), streptomycin (50 μg/ml) and 100 μg/ml of OPI (Sigma) was used as a standard medium for primary culture. Primary tumor cells were prepared from fresh human neuroblastoma tissues by a standard method. A total of 5×10^5 cells of each sample were resuspended in 1 ml of the standard medium, and seeded on 24-well tissue culture plates precoated with collagen. The cells were treated with or without ATRA at a final concentration of 5 μM for at least 2 weeks. The effects of ATRA on the growth and neurite extension of primary neuroblastoma cells were examined by phase-contrast microscope.

RNA extraction and RT–PCR

Total RNA was prepared from fresh-frozen tissues of primary neuroblastomas or cultured cells by using RNeasy Mini Kit (Qiagen, Valencia, CA, USA). Total RNA (2 μg) was reverse transcribed by using random primers and SuperScript II reverse transcriptase (Invitrogen, Carlsbad, CA, USA). The resultant cDNA was subjected to PCR-based amplification. The oligonucleotide primers used in this study were as follows: *bcl-2*, 5′-GAGGATTGTGGCCTTCTTTG-3′ (forward) and 5′-ACAGTTCCACAAAGGCATCC-3′ (reverse), and glyceraldehyde-3-phosphate dehydrogenase (*GAPDH*), 5′-ACCTGACCTGCCGTCTAGAA-3′ (forward) and 5′-TCCACCACCCTGTTGCTGTA-3′ (reverse). PCR products were electrophoretically separated on 1% neutral agarose gels and visualized by ethidium bromide staining.

Acknowledgements

We are grateful to the hospitals and institutions that provided us with surgical specimens. We thank Hideki Yamamoto and Atsushi Kawasaki for valuable discussions, and Yuki Nakamura for excellent technical assistance. This work was supported in part by a Grant-in-Aid from the Ministry of Health, Labour and Welfare for Third Term Comprehensive Control Research for Cancer, and a Grant-in-Aid for Scientific Research on Priority Areas and a Grant-in-Aid for Scientific Research (C) from the Ministry of Education, Culture, Sports, Science and Technology, Japan.

References

Abel F, Sjoberg RM, Nilsson S, Kogner P, Martinsson T. (2005). *Eur J Cancer* **41**: 635–646.
Antonsson B. (2001). *Cell Tissue Res* **306**: 347–361.
Balmer JE, Blomhoff R. (2002). *J Lipid Res* **43**: 1773–1808.
Brodeur GM. (2003). *Nat Rev Cancer* **3**: 203–216.
Brodeur GM, Nakagawara A. (1992). *Am J Pediatr Hematol Oncol* **14**: 111–116.
Cory S, Huang DC, Adams JM. (2003). *Oncogene* **22**: 8590–8607.
Culmsee C, Mattson MP. (2005). *Biochem Biophys Res Commun* **331**: 761–777.
Degterev A, Boyce M, Yuan J. (2003). *Oncogene* **22**: 8543–8567.
Dole M, Nunez G, Merchant AK, Maybaum J, Rode CK, Bloch CA *et al.* (1994). *Cancer Res* **54**: 3253–3259.
Encinas M, Iglesias M, Llecha N, Comella JX. (1999). *J Neurochem* **73**: 1409–1421.
Freemantle SJ, Spinella MJ, Dmitrovsky E. (2003). *Oncogene* **22**: 7305–7315.
Gallo G, Giarnieri E, Bosco S, Cappelli C, Alderisio M, Giovagnoli MR *et al.* (2003). *Anticancer Res* **23**: 777–784.
Kim R, Emi M, Tanabe K, Toge T. (2004). *Cancer* **101**: 2491–2502.
Lee MH, Nikolic M, Baptista CA, Lai E, Tsai LH, Massague J. (1996). *Proc Natl Acad Sci USA* **93**: 3259–3263.
Lippman SM, Lotan R. (2000). *J Nutr* **130**: 479S–482S.
Lombet A, Zujovic V, Kandouz M, Billardon C, Carvajal-Gonzalez S, Gompel A *et al.* (2001). *Eur J Biochem* **268**: 1352–1362.
Lopez-Carballo G, Moreno L, Masia S, Perez P, Barettino D. (2002). *J Biol Chem* **277**: 25297–25304.
Maden M. (2001). *Int Rev Cytol* **209**: 1–77.
Matthay KK, Villablanca JG, Seeger RC, Stram DO, Harris RE, Ramsay NK *et al.* (1999). *N Engl J Med* **341**: 1165–1173.
McCaffery PJ, Adams J, Maden M, Rosa-Molinar E. (2003). *Eur J Neurosci* **18**: 457–472.
Melino G, Thiele CJ, Knight RA, Piacentini M. (1997). *J Neurooncol* **31**: 65–83.
Morishima N, Nakanishi K, Takenouchi H, Shibata T, Yasuhiko Y. (2002). *J Biol Chem* **277**: 34287–34294.
Nagai J, Yazawa T, Okudela K, Kigasawa H, Kitamura H, Osaka H. (2004). *Cancer Res* **64**: 7910–7917.
Nakagawa T, Zhu H, Morishima N, Li E, Xu J, Yankner BA *et al.* (2000). *Nature* **403**: 98–103.
Nakagawara A. (1998). *Hum Cell* **11**: 115–124.
Nakagawara A, Arima-Nakagawara M, Scavarda NJ, Azar CG, Cantor AB, Brodeur GM. (1993). *N Engl J Med* **328**: 847–854.
Nakagawara A, Azar CG, Scavarda NJ, Brodeur GM. (1994). *Mol Cell Biol* **14**: 759–767.
Nakagawara A, Nakamura Y, Ikeda H, Hiwasa T, Kuida K, Su MS *et al.* (1997). *Cancer Res* **57**: 4578–4584.
Nakamura Y, Ozaki T, Koseki H, Nakagawara A, Sakiyama S. (2003). *Biochem Biophys Res Commun* **307**: 206–213.
Nikolaev AY, Li M, Puskas N, Qin J, Gu W. (2003). *Cell* **112**: 29–40.
Okuno S, Saito A, Hayashi T, Chan PH. (2004). *J Neurosci* **24**: 7879–7887.
Oltersdorf T, Elmore SW, Shoemaker AR, Armstrong RC, Augeri DJ, Belli BA *et al.* (2005). *Nature* **435**: 677–681.
Ostermeyer AG, Runko E, Winkfield B, Ahn B, Moll UM. (1996). *Proc Natl Acad Sci USA* **93**: 15190–15194.
Piacentini M, Annicchiarico-Petruzzelli M, Oliverio S, Piredda L, Biedler JL, Melino G. (1992). *Int J Cancer* **52**: 271–278.
Puthalakath H, Villunger A, O'Reilly LA, Beaumont JG, Coultas L, Cheney RE *et al.* (2001). *Science* **293**: 1829–1832.
Reynolds CP, Lemons RS. (2001). *Hematol Oncol Clin N Am* **15**: 867–910.
Romani P, Lu QL. (1994). *J Pathol* **172**: 273–278.
Schor NF. (1999). *J Neurooncol* **41**: 159–166.
Shi L, Gong S, Yuan Z, Ma C, Liu Y, Wang C *et al.* (2004). *Neurosci Lett* **375**: 7–12.
Takada N, Isogai E, Kawamoto T, Nakanishi H, Todo S, Nakagawara A. (2001). *Med Pediatr Oncol* **36**: 122–126.
Teitz T, Wei T, Valentine MB, Vanin EF, Grenet J, Valentine VA *et al.* (2000). *Nat Med* **6**: 529–535.
Thiele CJ, Reynolds CP, Israel MA. (1985). *Nature* **313**: 404–406.
Van Noesel MM, Van Bezouw S, Voute PA, Herman JG, Pieters R, Versteeg R. (2003). *Genes Chromosomes Cancer* **38**: 226–233.
Van Noesel MM, Versteeg R. (2004). *Gene* **325**: 1–15.
Villablanca JG, Khan AA, Avramis VI, Seeger RC, Matthay KK, Ramsay NK *et al.* (1995). *J Clin Oncol* **13**: 894–901.
Wang JL, Liu D, Zhang ZJ, Shan S, Han X, Srinivasula SM *et al.* (2000). *Proc Natl Acad Sci USA* **97**: 7124–7129.

Available online at www.sciencedirect.com
SCIENCE DIRECT®
ELSEVIER
Biochemical and Biophysical Research Communications 347 (2006) 327–333
BBRC
www.elsevier.com/locate/ybbrc

p73-dependent induction of 14-3-3σ increases the chemo-sensitivity of drug-resistant human breast cancers

Meixiang Sang [a,b], Yuanyuan Li [a], Toshinori Ozaki [a], Sayaka Ono [c], Kiyohiro Ando [a], Hideki Yamamoto [a], Tadayuki Koda [c], Cuizhi Geng [b], Akira Nakagawara [a,*]

[a] *Division of Biochemistry, Chiba Cancer Center Research Institute, Chiba 260-8717, Japan*
[b] *The First Surgery, Graduate School of Hebei Medical University, Hebei 050017, PR China*
[c] *Center for Functional Genomics, Hisamitsu Pharmaceutical Co., Inc., Chiba 260-8717, Japan*

Received 10 June 2006
Available online 21 June 2006

Abstract

It has been well documented that tumor suppressor *p53* is mutated in about 50% of all human tumors. *p53* status might be one of the critical determinants for the chemo-sensitivity of human tumors. In the present study, we have found that p53 family member p73 as well as 14-3-3σ is down-regulated in response to adriamycin (ADR) in ADR-resistant human breast cancer-derived MBA-MD-436 cells which carry *p53* mutation. Like p53, *14-3-3σ* was transactivated by p73 and, in turn, stabilized p73. Luciferase reporter analysis and colony formation assays demonstrated that 14-3-3σ has an ability to enhance the p73-mediated transcriptional activity as well as its pro-apoptotic function. Furthermore, enforced expression of 14-3-3σ increased the ADR sensitivity of MBA-MD-436 cells. Taken together, our present results strongly suggest that p73-dependent induction of 14-3-3σ plays an important role in the regulation of chemo-sensitivity of breast cancers bearing *p53* mutation.

Keywords: Adriamycin; Breast cancer; 14-3-3σ; p53; p73

The tumor suppressor *p53* which encodes a sequence-specific nuclear transcription factor is the most frequently mutated gene in human cancers [1]. Mounting evidence showed that p53 is induced to be accumulated in response to various cellular stresses such as DNA damage, and thereby exerts its pro-apoptotic function through the transactivation of the p53-target genes implicated in the regulation of the apoptotic cell death including *Bax*, *Noxa*, *Puma*, and *p53AIP1* [2–5]. Newly identified p53 family members, p73 and p63, promote cell cycle arrest and/or apoptosis similarly to p53 [6–10]. Although *p73* and *p63* are rarely mutated in human cancers [11], it has been shown that they are required for the p53-mediated apoptosis in response to DNA damage [12]. Since cancer cells which carry *p53* mutation are more resistant to chemotherapeutic agents than those with wild-type p53 [13,14], it is likely that p73 and/or p63 might contribute to sensitize p53-deficient cancer cells to chemotherapeutic agents.

About 30–50% of human breast cancers express mutant forms of p53 [15,16]. Additionally, Moll et al. found that the pro-apoptotic function of wild-type p53 expressed in about 30% of human breast cancers is inhibited due to its aberrant cytoplasmic localization [17]. 14-3-3σ, which is one of the 14-3-3 family members, has been initially identified as a human mammary epithelium-specific marker 1 [18]. Intriguingly, the expression of 14-3-3σ is undetectable in most breast cancers due to the hypermethylation of CpG islands in the *14-3-3σ* gene [19]. Enforced expression of 14-3-3σ suppresses the anchorage-independent growth of several breast cancer cell lines [20]. Alternatively, it has been shown that 14-3-3σ is strongly induced in response to DNA damage, and its expression is directly regulated by

* Corresponding author. Fax: +81 43 265 4459.
E-mail address: akiranak@chiba-cc.jp (A. Nakagawara).

0006-291X/$ - see front matter © 2006 Elsevier Inc. All rights reserved.
doi:10.1016/j.bbrc.2006.06.079

p53 [21]. Yang et al. described that 14-3-3σ stabilizes p53 and enhances its transcriptional activity through the interaction with p53, suggesting that 14-3-3σ has a positive feedback effect on p53 [22].

In the present study, we have found that the adriamycin (ADR)-resistant phenotype of certain human breast cancer cells with *p53* mutation is significantly associated with the down-regulation of 14-3-3σ as well as p73. Of note, *14-3-3σ* was transactivated by p73, and enhanced its transcriptional and pro-apoptotic activity. Thus, it is likely that p73/14-3-3σ pathway plays an important role in the regulation of DNA damage-induced apoptosis in certain breast cancer cells bearing *p53* mutation.

Materials and methods

Cell culture and transfection. COS7 and human breast cancer-derived cell lines were maintained in Dulbecco's modified Eagle's medium (DMEM) supplemented with 10% heat-inactivated fetal bovine serum (FBS, Invitrogen) and antibiotic mixture. p53-deficient human lung carcinoma H1299 cells were grown in RPMI 1640 medium plus 10% heat-inactivated FBS and antibiotic mixture. Cultures were grown at 37 °C in a water-saturated atmosphere of 5% CO_2 in air. For transfection, cells were transfected with the indicated combinations of the expression plasmids using LipofectAMINE 2000 transfection reagent according to the manufacturer's recommendations (Invitrogen).

MTT assays. Cells were seeded at a cell density of 5000 cells/well in 96-well tissue culture plates. After attachment overnight, cells were exposed to adriamycin (ADR) at a final concentration of 1 μM for the indicated time periods. MTT assays were performed as described previously [23]. In brief, 10 μl of MTT solution was added to each well. After one hour of incubation at 37 °C, the absorbance readings for each well were carried out at 570 nm using the microplate reader (Bio-Rad).

TUNEL assays. Transfected cells were exposed to ADR at a final concentration of 1 μM for 24 h. Apoptotic cells were identified using an *in situ* cell detection, peroxidase kit (Roche Applied Science). In brief, cells were washed with ice-cold PBS and fixed in 4% paraformaldehyde for 1 h. Cells were then permeabilized with 0.1% Triton X-100 in 0.1% sodium citrate for 2 min on ice and washed with PBS. The labeling reaction was performed using TMR red-labeled dUTP together with other nucleotides by terminal deoxynucleotidyl transferase for 1 h in the dark at 37 °C in a humidified chamber. Then cells were washed with PBS, mounted, and the incorporated TMR red-labeled dUTP was analyzed using a Fluoview laser scanning confocal microscope (Olympus).

RT-PCR. Total RNA was extracted from the indicated cell lines by using RNeasy Mini Kit (Qiagen) according to the manufacturer's protocol. cDNA was generated from 1 μg of total RNA using random primers and SuperScript II reverse transcriptase (Invitrogen). PCR-based amplification was performed using the cDNA as a template with the following primers: *p73* forward, 5′-TGGAACCAGACAGCACCTACTTCG-3′ and *p73* reverse, 5′-TGCTGGAAAGTGACCTCAAAGTGG-3′; $p21^{WAF1}$ forward, 5′-ATGAAATTCACCCCCTTTCC-3′ and $p21^{WAF1}$ reverse, 5′-CCCTAATCACCTGCCTGACCATTCCACCAAGG-3′; *erbB2* forward, 5′-GGGCTGGCCCGATGTATTTGAT-3′ and *erbB2* reverse, 5′-ATAGAGGTTGTCGAAGGCTGGGC3′; *Noxa* forward, 5′-CTGGAAGTCGAGTGTGCTACT-3′ and *Noxa* reverse, 5′-TCAGGTTCCTGAGCAGAAGAG-3′; *14-3-3σ* forward, 5′-GAGCGAAACCTGCTCTCAGT-3′ and *14-3-3σ* reverse, 5′-CTCCTTGATGAGGTGGCTGT-3′; *GAPDH* forward, 5′-ACCTGACCTGCCGTCTAGAA-3′ and *GAPDH* reverse, 5′-TCCACCACCCTGTTGCTGTA-3′. PCR products were separated on 2% agarose gel electrophoresis and visualized by ethidium bromide staining.

Immunoblotting. Whole cell lysates were separated on 10% SDS–PAGE and transferred onto a polyvinylidene difluoride membrane (Millipore). The membrane was blocked with TBS (50 mM Tris–HCl, pH 8.0, 100 mM NaCl and 0.1% Tween 20) containing 5% nonfat dried milk, and then probed with the monoclonal anti-p73 (Ab-4, NeoMarkers), monoclonal anti-erbB2 (3B5, Calbiochem), polyclonal anti-14-3-3σ (C-18, Santa Cruz Biotechnology), polyclonal anti-Noxa (Zymed), or with polyclonal anti-actin (20-33, Sigma) antibody. The immunoreactive bands were visualized by using HRP-conjugated anti-mouse or anti-rabbit IgG antibody (Jackson ImmunoResearch Laboratories) and ECL (Amersham Biosciences).

Immunoprecipitation. Whole cell lysates prepared from MBA-MD-436 cells treated with or without ADR were immunoprecipitated with the monoclonal anti-p73 followed by immunoblotting with the anti-p73 antibody.

Protein decay rate analysis. COS7 cells were transiently transfected with the indicated combinations of the expression plasmids. Twenty-four hours after transfection, cells were exposed to cycloheximide (Sigma) at a final concentration of 100 μg/ml. At the indicated time points after the treatment with cycloheximide, cells were harvested and subjected to immunoblotting with the anti-p73 or with the anti-actin antibody.

Luciferase reporter assay. p53-deficient H1299 cells were transiently transfected with 100 ng of the p53/p73-responsive luciferase reporter plasmid ($p21^{WAF1}$ or *BAX*), 10 ng of pRL-TK *Renilla* luciferase cDNA, and 25 ng of the expression plasmid for HA-p73α together with or without the increasing amounts of the expression plasmid encoding 14-3-3σ. Total amounts of plasmid DNA were kept constant (510 ng) with pcDNA3 (Invitrogen) per transfection. Forty-eight hours after transfection, both firefly and *Renilla* luciferase activities were measured by the dual-luciferase reporter assay system according to the manufacturer's instructions (Promega). The firefly luminescence signal was normalized based on the *Renilla* luminescence signal. The results were obtained from at least three sets of transfection and presented as means ± SD.

Colony formation assay. H1299 cells were seeded at a cell density of 2×10^5 cells/well in 6-well tissue culture plates and transfected with the indicated combinations of the expression plasmids. Forty-eight hours after transfection, cells were selected with G418 (at a final concentration of 400 μg/ml) for 2 weeks. The surviving colonies were fixed in methanol and stained with Giemsa's solution.

Results

ADR sensitivity and expression of p53-related genes in human breast cancer-derived cell lines

To examine the adriamycin (ADR) sensitivity of the human breast cancer-derived cell lines including MCF-7, MDA-MB-231, and MDA-MB-436, these cells were treated with 1 μM of ADR for the indicated time periods, and their viabilities were analyzed by the standard MTT assay. ADR has been considered as a mandatory agent in breast cancer chemotherapy [24]. As described previously [25], MCF-7 cells carry wild-type p53, whereas MDA-MB-231 and MDA-MB-436 cells express mutant form of p53. As shown in Fig. 1A, MCF-7 and MDA-MB-231 cells underwent apoptotic cell death in response to ADR, whereas MDA-MB-436 cells showed an ADR-resistant phenotype, which was also supported by FACS analysis (data not shown). Consistent with the previous observations [1], p53 was induced to be accumulated at protein level in MCF-7 cells exposed to ADR in association with the up-

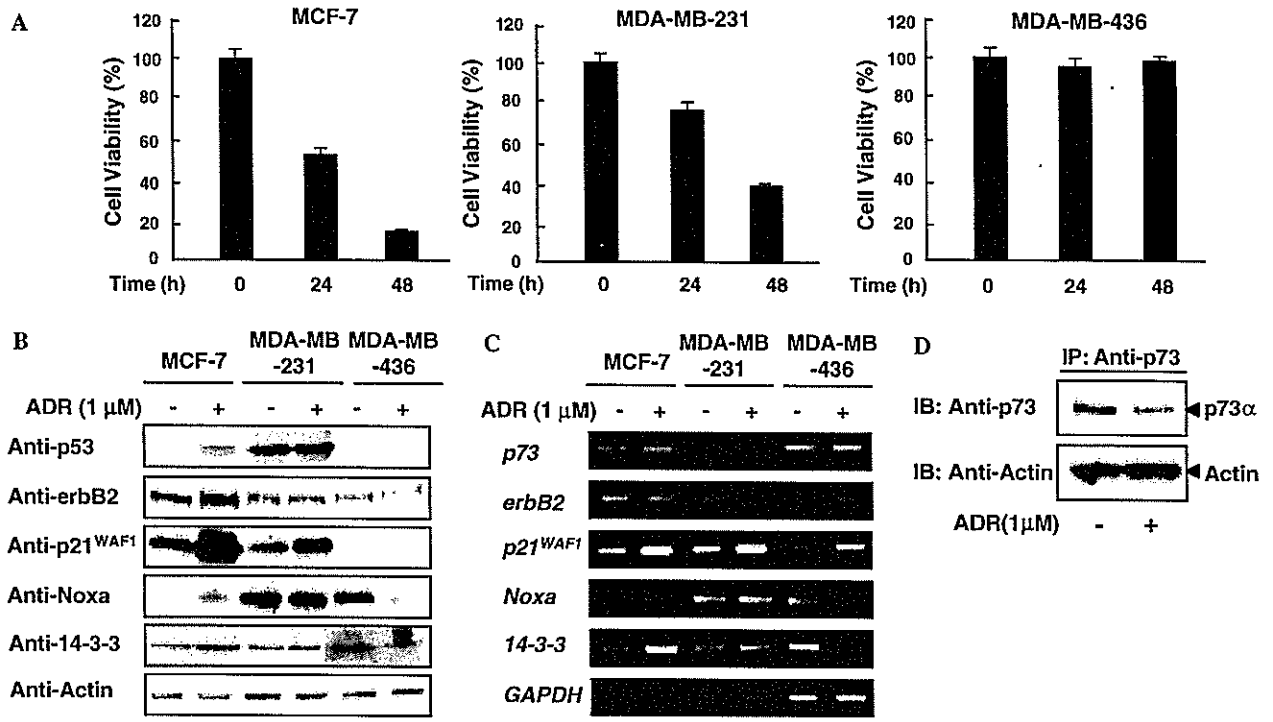

Fig. 1. The expression of *p53*-related genes in breast cancer cells in response to ADR. (A) Cell survival assays. Human breast cancer-derived MCF-7, MDA-MB-231, and MDA-MB-436 cells were exposed to ADR (at a final concentration of 1 μM). At the indicated time periods after the treatment with ADR, cell viability was examined by standard MTT assay. (B) Immunoblotting. MCF-7, MDA-MB-231, and MDA-MB-436 cells were treated with ADR (at a final concentration of 1 μM) or left untreated. Whole cell lysates were prepared and processed for immunoblotting with the indicated antibodies. Immunoblotting for actin is shown as control for protein loading. (C) RT-PCR analysis. MCF-7, MDA-MB-231, and MDA-MB-436 cells were treated with ADR as in (B). Twenty-four hours after the treatment, total RNA was prepared and subjected to RT-PCR for the expression of *p73*, *erbB2*, *p21*^{WAF1}, *Noxa* and *14-3-3σ*. Amplification of *GAPDH* served as an internal control. (D) Immunoprecipitation. MDA-MB-436 cells were treated with 1 μM ADR or left untreated. Twenty-four hours after the treatment, whole cell lysates were immunoprecipitated with the monoclonal anti-p73 antibody followed by immunoblotting with the anti-p73 antibody.

regulation of its direct targets such as p21^{WAF1}, Noxa, and 14-3-3σ (Fig. 1B). In ADR-sensitive MDA-MB-231 cells, ADR-mediated increase in the amounts of p21^{WAF1} was detectable, however, the expression levels of p53, Noxa, and 14-3-3σ remained unchanged regardless of ADR treatment, suggesting that ADR-mediated apoptotic cell death in MDA-MB-231 cells might be regulated in a p53-independent manner. In a sharp contrast to MCF-7 and MDA-MB-231 cells, p53 was undetectable under our experimental conditions, and ADR-dependent down-regulation of Noxa and 14-3-3σ was observed in ADR-resistant MDA-MB-436 cells. Similar results were also obtained in RT-PCR analysis (Fig. 1C). *p73* as well as *erbB2* mRNA level remained almost constant regardless of ADR treatment. In addition, ADR had no detectable effects of the expression levels of *p53* mRNA (data not shown). Of note, immunoprecipitation experiments demonstrated that p73 is reduced in MDA-MB-436 cells exposed to ADR (Fig. 1D), whereas p73 levels remained unchanged in MCF-7 and MBA-MD-231 cells regardless of ADR treatment (data not shown), indicating that ADR-mediated down-regulation of Noxa and 14-3-3σ could be due to the down-regulation of p73, and also suggesting that p73 could play an important role in the regulation of ADR sensitivity in certain breast cancer cells bearing *p53* mutation.

14-3-3σ is a direct target of p73 and increases its stability

Since Noxa has been shown to be a direct transcriptional target of p53 as well as p73, and play a critical role in the regulation of p53/p73-mediated apoptotic cell death [9], we focused our attention on the possible link between p73 and 14-3-3σ. Recently, Yang et al. demonstrated that 14-3-3σ is a direct transcriptional target of p53 and increases its stability [22]. Thus, we sought to examine whether p73 could transactivate *14-3-3σ* in cells. COS7 cells were transiently transfected with the expression plasmid for HA-p73α or p53. Forty-eight hours after transfection, total RNA was prepared and subjected to RT-PCR analysis. As shown in Fig. 2A, HA-p73α as well as p53 enhanced the transcription of the endogenous *14-3-3σ*. Similar results were also obtained in immunoblotting (Fig. 2B). Next, we examined the possible effect of 14-3-3σ on the stability of p73α. To this end, p53-deficient H1299 cells were transiently co-transfected with the constant amount of the HA-p73α expression plasmid along with or without the increasing amounts of the expression plasmid for 14-3-3σ. As seen

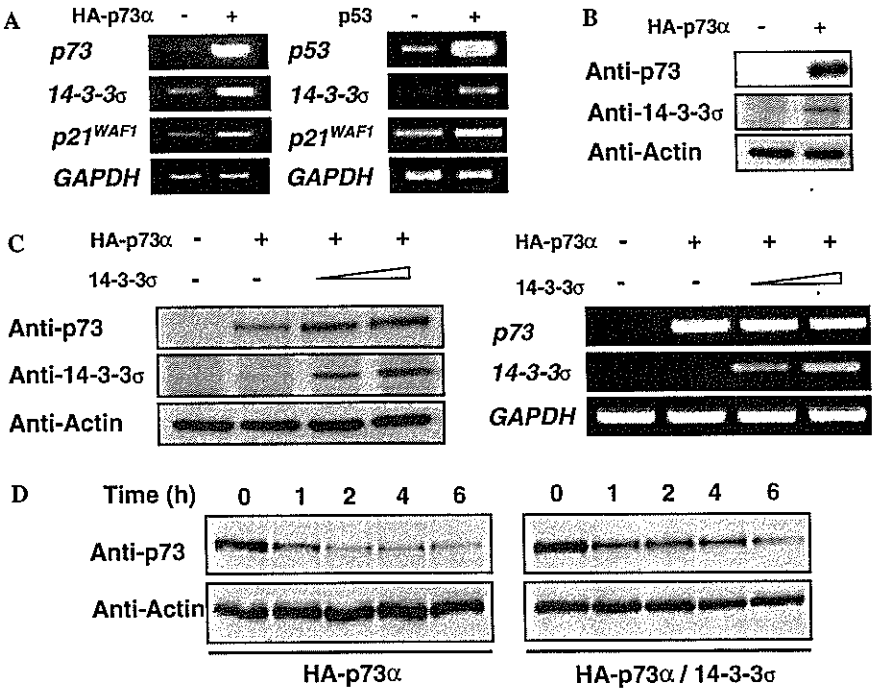

Fig. 2. *14-3-3σ* is a transcriptional target of p73 and increases its stability. (A) p73-mediated up-regulation of 14-3-3σ. COS7 cells were transiently transfected with the expression plasmid for HA-p73α (left panel) or p53 (right panel). Forty-eight hours after transfection, total RNA was prepared and subjected to RT-PCR. (B) Immunoblotting. p53-deficient H1299 cells were transiently transfected with the empty plasmid or with the expression plasmid encoding HA-p73α. Forty-eight hours after transfection, whole cell lysates were prepared and subjected to immunoblotting with the indicated antibodies. (C) 14-3-3σ stabilizes p73. H1299 cells were transiently co-transfected with the constant amount of HA-p73α expression plasmid together with or without the increasing amounts of the expression plasmid for 14-3-3σ. Forty-eight hours after transfection, whole cell lysates and total RNA were analyzed by immunoblotting with the indicated antibodies and RT-PCR, respectively. (D) A half-life of p73 in the presence of 14-3-3σ. H1299 cells were transiently transfected with the HA-p73α expression plasmid alone or with the HA-p73α expression plasmid plus 14-3-3σ expression plasmid. Twenty-four hours after transfection, cells were exposed to cycloheximide (at a final concentration of 100 μg/ml). At the indicated time points after the addition of cycloheximide, whole cell lysates were analyzed for HA-p73α. Actin was used for equal protein loading.

in Fig. 2C, 14-3-3σ increased the amounts of HA-p73α in a dose-dependent manner, whereas 14-3-3σ had undetectable effect on the *p73α* mRNA level, suggesting that 14-3-3σ has an ability to stabilize p73 in cells. To further confirm this notion, we measured a half-life of p73α in the presence or absence of the exogenous 14-3-3σ using cycloheximide blockade. As seen in Fig. 2D, a half-life of p73α was prolonged in the presence of 14-3-3σ as compared with that of p73α alone. Taken together, our present results strongly suggest that, like p53, 14-3-3σ is a direct transcriptional target of p73 and stabilizes p73.

14-3-3σ enhances the p73-mediated transcriptional activity as well as pro-apoptotic function

To address whether 14-3-3σ could affect the p73 function, we performed the luciferase reporter assays. For this purpose, H1299 cells were transiently co-transfected with the constant amount of the p73α expression plasmid and the p53/p73-responsive luciferase reporter construct carrying the $p21^{WAF1}$ or *Bax* promoter together with or without the increasing amounts of the expression plasmid for 14-3-3σ. Forty-eight hours after transfection, cells were harvested and their luciferase activities were measured. As expected, 14-3-3σ enhanced the p73α-mediated transactivation toward $p21^{WAF1}$ and *Bax* promoters in a dose-dependent manner (Fig. 3A). Next, we examined whether 14-3-3σ could enhance the p73-mediated apoptosis. H1299 cells were transfected with the empty plasmid, HA-p73α expression plasmid, or with the HA-p73α expression plasmid plus 14-3-3σ expression plasmid. Forty-eight hours after transfection, cells were transferred to the fresh medium containing G418. After 2 weeks of selection, G418-resistant colonies were stained with Giemsa's solution. As shown in Fig. 3B, the number of G418-resistant colonies was significantly reduced in cells co-expressing HA-p73α and 14-3-3σ as compared with that in cells expressing HA-p73α alone. Thus, we concluded that 14-3-3σ has an ability to enhance the p73 function through the stabilization of p73.

Enforced expression of 14-3-3σ increases the ADR sensitivity of ADR-resistant MDA-MB-436 cells

To ask whether 14-3-3σ could affect the ADR sensitivity in ADR-resistant MDA-MB-436 cells, MDA-MB-436 cells were transfected with the empty plasmid (436-C) or with the expression plasmid for 14-3-3σ (436-14), and maintained in the presence of G418. Two weeks of selection,

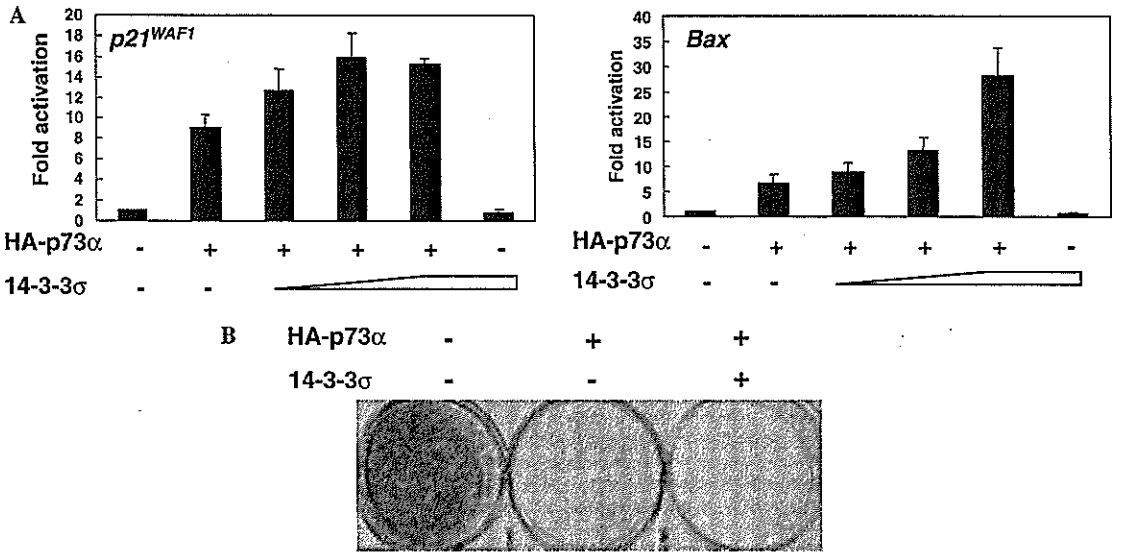

Fig. 3. *14-3-3σ* enhances the p73-mediated transcription as well as apoptosis. (A) Luciferase reporter assay. H1299 cells were transiently co-transfected with the constant amounts of the expression plasmid for HA-p73α, p53/p73-responsive luciferase reporter construct containing the $p21^{WAF1}$ (left panel) or *Bax* (right panel) promoter, *Renilla* luciferase reporter together with or without the increasing amounts of the expression plasmid for 14-3-3σ. Forty-eight hours after transfection, luciferase activities were measured as described under "Materials and methods". (B) Colony formation assay. H1299 cells were transfected with empty plasmid, the expression plasmid for HA-p73α or with the expression plasmid for HA-p73α plus 14-3-3σ expression plasmid. Forty-eight hours after transfection, cells were transferred to the fresh medium containing G418 (at a final concentration of 400 μg/ml). After 2 weeks of selection, drug-resistant colonies were fixed and stained with Giemsa's solution.

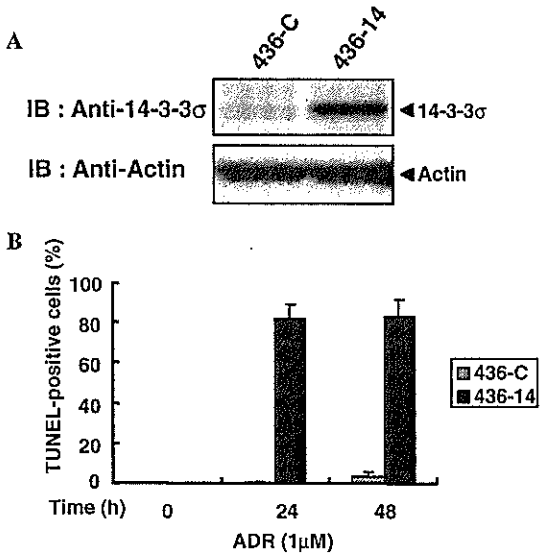

Fig. 4. Effects of 14-3-3σ on the ADR sensitivity in MDA-MB-436 cells. (A) Enforced expression of 14-3-3σ in MDA-MB-436 cells. MDA-MB-436 cells were transfected with the empty plasmid (436-C) or with the expression plasmid for 14-3-3σ (436-14). Forty-eight hours after transfection, cells were transferred to the fresh medium containing 400 μg/ml G418. After 2 weeks of selection, surviving cells were harvested and then whole cell lysates were subjected to immunoblotting with the indicated antibodies. (B) TUNEL assay. Control MDA-MB-436 cells (436-C) and MDA-MB-436 cells expressing 14-3-3σ (436-14) were exposed to ADR (at a final concentration of 1 μg/ml) or left untreated. Twenty-four and Forty-eight hours after the treatment with ADR, apoptotic cell death was examined by TUNEL assay.

whole cell lysates were prepared from the surviving cells and subjected to immunoblotting. As shown in Fig. 4A, the increased expression of 14-3-3σ was observed in cells transfected with 14-3-3σ expression plasmid. We then examined the ADR sensitivity by TUNEL assays. As seen in Fig. 4B, the number of MDA-MB-436 cells expressing 14-3-3σ with apoptotic nuclei was significantly increased in response to ADR as compared with that of the control MDA-MB-436 cells. Collectively, our present results strongly suggest that p73/14-3-3σ pathway plays an important role in the regulation of the chemo-sensitivity of certain breast cancer cells bearing *p53* mutation.

Discussion

Mammalian 14-3-3 protein family comprises at least seven isoforms. Among them, *14-3-3σ* is mapped at human chromosome 1p35, a region which shows frequent loss of heterozygosity in a wide variety of human cancers including breast cancers [21,26]. Indeed, the expression levels of *14-3-3σ* were significantly lower in breast cancers than those in normal breast epithelium, which might be due to the hypermethylation of CpG islands in the *14-3-3σ* gene locus [19], and an enforced expression of 14-3-3σ inhibited the oncogene-activated tumorigenesis [27]. Intriguingly, 14-3-3σ was transactivated by p53 in response to DNA damage [21], and positively regulated its activity [22], indicating that there exists a positive feedback regulation of p53 by its target 14-3-3σ. In the present study, we have found that 14-3-3σ is a direct

transcriptional target of p73 and enhances the p73-mediated transcriptional as well as pro-apoptotic activity. Furthermore, an enforced expression of 14-3-3σ in ADR-resistant human breast cancer MDA-MB-436 cells bearing *p53* mutation resulted in an increased cell killing by ADR. Collectively, our present results strongly suggest that p73/14-3-3σ pathway plays an important role in the regulation of chemo-sensitivity in certain breast cancer cells bearing *p53* mutation.

According to the results described by Yang et al. 14-3-3σ had an ability to increase the stability and the transcriptional activity of p53 through the physical interaction with p53 [22]. They also demonstrated that 14-3-3σ inhibits the MDM2-mediated p53 ubiquitination and nuclear export. In spite of our extensive efforts, we could not detect the physical interaction between p73α and 14-3-3σ under our experimental conditions (data not shown). Although it might be due to the different cell systems used in our immunoprecipitation experiments, it is likely that 14-3-3σ-mediated increase in the stability and activity of p73α could be regulated by a still unknown indirect mechanism(s). Recently, Rossi et al. reported that a HECT-type E3 ubiquitin protein ligase Itch binds to and ubiquitinates p73, and thereby promoting its rapid proteasome-dependent degradation [28]. They also described that the expression levels of Itch are down-regulated in cells in response to DNA damage. Since 14-3-3σ induced the degradation of MDM2 [22], it is tempting to speculate that E3 ubiqitin protein ligase activity of Itch could be blocked by 14-3-3σ. This issue is currently under investigation.

According to the previous results, p73 was induced to be accumulated at protein level in response to ADR treatment and thereby promoting apoptotic cell death [29,30]. In a sharp contrast, p53/p73-target genes such as *Noxa* and *14-3-3σ* were significantly down-regulated following ADR treatment in ADR-resistant MDA-MB-436 cells. MCF-7 cells carrying wild-type p53 underwent apoptosis in response to ADR in a p53-dependent manner. Since MDA-MB-436 cells express nonfunctional p53 [25], it is possible that the ADR-mediated upstream activation pathways including the post-translational modifications such as phosphorylation and acetylation which regulate p73 function [9,10] might be disrupted in these cells. Based on our present results, enforced expression of 14-3-3σ in p53-deficient H1299 cells enhanced the p73-mediated apoptotic cell death as examined by colony formation assay. Furthermore, the ADR sensitivity of MDA-MB-436 cells was increased in the presence of exogenously expressed 14-3-3σ. Thus, it is likely that p73/14-3-3σ-mediated apoptotic pathway might be one of the critical determinants of cell fate in response to ADR in certain breast cancer cells bearing *p53* mutation, and that p73 might be effective in p53-deficient breast cancer cells which are resistant to anti-cancer drug. In this connection, further work is required to determine how the ADR-mediated activation of p73 is blocked in MDA-MB-436 cells.

Acknowledgments

This work was supported in part by a Grant-in-Aid from the Ministry of Health, Labor and Welfare for Third Term Comprehensive Control Research for Cancer, a Grant-in-Aid for Scientific Research on Priority Areas from the Ministry of Education, Culture, Sports, Science and Technology, Japan, and a Grant-in-Aid for Scientific Research from Japan Society for the Promotion of Science.

References

[1] K.H. Vousden, X. Lu, Live or death: the cells response to p53, Nat. Rev. Cancer 2 (2002) 594–604.
[2] T. Miyashita, J.C. Reed, Tumor suppressor p53 is a direct transcriptional activator of the human bax gene, Cell 80 (1995) 293–299.
[3] E. Oda, R. Ohki, H. Murasawa, J. nemoto, T. Shibue, T. Yamashita, T. Tokino, T. Taniguchi, N. Tanaka, Noxa, a BH3-only member of the Bcl-2 family and candidate mediator of p53-induced apoptosis, Science 288 (2000) 1053–1058.
[4] J. Yu, L. Zhang, P.M. Hwang, K.W. Kinzler, B. Vogelstein, PUMA induces the rapid apoptosis of colorectal cancer cells, Mol. Cell 7 (2001) 673–682.
[5] K. Oda, H. Arakawa, T. Tanaka, K. matsuda, C. Tanikawa, T. Mori, H. Nishimori, K. Tamai, T. Tokino, Y. Nakamura, Y. Taya, p53AIP1, a potential mediator of p53-dependent apoptosis, and its regulation by Ser-46- phosphorylated p53, Cell 102 (2000) 849–862.
[6] M. Kaghad, H. Bonnet, A. Yang, L. Creancier, J.C. Biscan, A. Valent, A. Minty, P. Chalon, J.M. Lelias, X. Dumont, P. Ferrara, F. McKeon, D. Caput, Monoallelically expressed gene related to p53 at 1p36, a region frequently deleted in neuroblastoma and other human cancers, Cell 90 (1997) 809–819.
[7] M. Osada, M. Ohba, C. Kawahara, C. Ishioka, R. Kanamaru, I. Kato, Y. Ikawa, Y. Nimura, A. Nakagawara, M. Obinata, S. Ikawa, Cloning and functional analysis of human p51, which structurally and functionally resembles p53, Nat. Med. 4 (1998) 839–843.
[8] A. Yang, M. Kaghad, Y. Wang, E. Gillett, M.D. Fleming, V. Dotsch, N.C. Andrews, D. Caput, F. McKeon, p63, a p53 homolog at 3q27-29, encodes multiple products with transactivating, death-inducing, and dominant-negative activities, Mol. Cell 2 (1998) 305–316.
[9] G. Melino, V. De Laurenzi, K.H. Vousden, p73: friend or foe in tumorigenesis, Nat. Rev. Cancer 2 (2002) 605–615.
[10] T. Ozaki, A. Nakagawara, p73, a sophisticated p53 family member in the cancer world, Cancer Sci. 96 (2005) 729–737.
[11] S. Ikawa, A. Nakagawara, Y. Ikawa, p53 family genes: structural comparison, expression and mutation, Cell Death Differ. 6 (1999) 1154–1161.
[12] E.R. Flores, K.Y. Tsai, D. Crowley, S. Sengupta, A. Yang, F. McKeon, T. Jacks, p63 and p73 are required for p53-dependent apoptosis in response to DNA damage, Nature 416 (2002) 560–564.
[13] D. Gallardo, K.E. Drazan, W.H. McBride, Adenovirus-based transfer of wild-type p53 gene increases ovarian tumor radiosensitivity, Cancer Res. 56 (1996) 4891–4893.
[14] T. Mukhopadhyay, J.A. Roth, Induction of apoptosis in human lung cancer cells after wild-type p53 activation by methoxyestradiol, Oncogene 14 (1997) 379–384.
[15] L.V. Crawford, D.C. Pim, P. Lamb, The cellular protein p53 in human tumours, Mol. Biol. Med. 2 (1984) 261–272.
[16] G. Cattoretti, F. Rilke, S. Andreola, L. D'Amato, D. Domenico, p53 in breast cancer, Int. J. Cancer 41 (1988) 178–183.
[17] U.M. Moll, G. Riou, A.J. Levine, Two distinct mechanisms alter p53 in breast cancer: mutation and nuclear exclusion, Proc. Natl. Acad. Sci. USA 89 (1992) 7262–7266.
[18] G.L. Prasad, E.M. Valverius, E. McDuffie, H.L. Cooper, Complementary DNA cloning of a novel epithelial cell marker protein,

Hmel, that may be down-regulated in neoplastic mammary cells, Cell Growth Differ. 3 (1992) 507–513.
[19] A.T. Ferguson, E. Evron, C.B. Umbricht, T.K. Pandita, T.A. Chan, H. Hermeking, J.R. Marks, A.R. Lambers, P.A. Futreal, M.R. Stampfer, S. Sukumar, High frequency of hypermethylation at the 14-3-3s locus leads to gene silencing in breast cancer, Proc. Natl. Acad. Sci. USA 97 (2000) 6049–6054.
[20] C. Laronga, H.Y. Yang, C. Neel, M.H. Lee, Association of the cyclin-dependent kinases and 14-3-3σ negatively regulates cell cycle progression, J. Biol. Chem. 275 (2000) 23106–23112.
[21] H. Hermeking, C. Lengauer, K. Polyak, T.C. He, L. Zhang, S. Thiagalingam, K.W. Kinzler, B. Vogelstein, 14-3-3σ is a p53-regulated inhibitor of G2/M progression, Mol. Cell 1 (1997) 3–11.
[22] H.-Y. Yang, Y.-Y. Wen, C.-H. Chen, G. Lozano, M.-H. Lee, 14-3-3σ positively regulates p53 and suppresses tumor growth, Mol. Cell. Biol. 23 (2003) 7096–7170.
[23] K. Ando, T. Ozaki, H. Yamamoto, K. Furuya, M. Hosoda, S. Hayashi, M. Fukuzawa, A. Nakagawara, Polo-like linase 1 (Plk1) inhibits p53 function by physical interaction and phosphorylation, J. Biol. Chem. 279 (2004) 25549–25561.
[24] M. Vayssade, H. Haddada, L. Faridoni-Laurens, S. Tourpin, A. Valent, J. Benard, J.C. Ahomadegbe, p73 functionally replaces p53 in adriamycin-treated, p53-deficient breast cancer cells, Int. J. Cancer 116 (2005) 860–869.
[25] J. Gray-Bablin, J. Zalvide, M.P. Fox, C.J. Knickerbocker, J.A. DeCaprio, K. Keyomarsi, Cyclin E, a redundant cyclin in breast cancer, Proc. Natl. Acad. Sci. USA 93 (1996) 15215–15220.
[26] G. Ragnarsson, G. Eiriksodottir, J.T. Johannsdottir, J.G. Jonasson, V. Egilsson, S. Ingvarsson, Loss of heterozygosity at chromosome 1p in different solid human tumours: association with survival, Br. J. Cancer 79 (1999) 1468–1474.
[27] H. Yang, R. Zhao, M.-H. Lee, 14-3-3σ, a p53 regulator, suppresses tumor growth of nasopharyngeal carcinoma, Mol. Cancer Ther. 5 (2006) 253–260.
[28] M. Rossi, V. De Laurenzi, E. Munarriz, D.R. Green, Y.C. Liu, K.H. Vousden, G. Cesareni, G. Melino, The ubiquitin-protein ligase Itch regulates p73 stability, EMBO J. 24 (2005) 836–848.
[29] A. Costanzo, P. Merlo, N. Pediconi, M. Fulco, V. Sartorelli, P.A. Cole, G. Fontemaggi, M. Fanciulli, L. Schiltz, G. Blandino, C. Balsano, M. Levrero, DNA damage-dependent acetylation of p73 dictates the selective activation of apoptotic target genes, Mol. Cell 9 (2002) 175–186.
[30] M.S. Irwin, K. Kondo, M.C. Marin, L.S. Cheng, W.C. Hahn, W.G. Kaelin Jr., Chemosensitivity linked to p73 function, Cancer Cell 3 (2003) 403–410.

Available online at www.sciencedirect.com
ScienceDirect
Biochemical and Biophysical Research Communications 351 (2006) 57–63
BBRC
www.elsevier.com/locate/ybbrc

The intracellular domain of the amyloid precursor protein (AICD) enhances the p53-mediated apoptosis

Toshinori Ozaki [a,1], Yuanyuan Li [a,1], Hironobu Kikuchi [a], Taisuke Tomita [b], Takeshi Iwatsubo [b], Akira Nakagawara [a,*]

[a] *Division of Biochemistry, Chiba Cancer Center Research Institute, Chiba 260-8717, Japan*
[b] *Department of Neuropathology and Neuroscience, Graduate School of Pharmaceutical Sciences, University of Tokyo, Tokyo 113-0033, Japan*

Received 29 September 2006
Available online 9 October 2006

Abstract

Amyloid precursor protein (APP)-derived intracellular domain (AICD) has a cytotoxic effect on neuronal cells and also participates in the regulation of gene transactivation. However, the precise molecular mechanisms behind the AICD-mediated apoptosis remain unknown. In this study, we have demonstrated that AICD interacts with p53 and enhances its transcriptional and pro-apoptotic functions. p53 was induced to be accumulated and associated with APP in response to cisplatin. Indeed, APP-C57 was co-immunoprecipitated with the endogenous p53. Enforced expression of APP-C57 or APP-C59 in U2OS cells bearing wild-type p53 led to an increase in number of apoptotic cells, whereas they had undetectable effects on p53-deficient H1299 cells, suggesting that AICD contributes to the activation of the p53-mediated apoptotic pathway. Consistent with this notion, the p53-mediated transcriptional activation and apoptosis were significantly enhanced by co-expression with APP-C57 or APP-C59. Thus, our present results strongly suggest that AICD triggers apoptosis through the p53-dependent mechanisms.

Keywords: AICD; Apoptosis; APP; Fe65; γ-Secretase; p53

Amyloid precursor protein (APP) is a type I transmembrane glycoprotein with a large extracellular domain, a single hydrophobic transmembrane region, and a short cytoplasmic tail [1]. APP is cleaved sequentially by α-, β-, and γ-secretases, which results in the generation of the large soluble NH_2-terminal ectodomain, small hydrophobic extracellular amyloid-β (Aβ, 40- and 42-residues) peptide, and APP intracellular domain (AICD, 57- and 59-residue-long COOH-terminal fragments) [2]. Among them, Aβ has been believed to be one of the major neurodegenerative agents in Alzheimer's disease (AD) [3]. Indeed, Aβ rapidly aggregates into fibrils and the extracellular fibrillar Aβ can promote apoptosis in cultured neurons [4]. Alternatively, AICD has been initially identified in brains of AD patients [5] and AICD itself induced apoptosis in human H4 neuroglioma cells [6]. However, the precise molecular mechanisms by which AICD exerts its pro-apoptotic activity remain to be determined. It has been shown that AICD is stabilized and translocated into the nucleus by collaboration with the adaptor protein Fe65 [6–8], raising a possibility that APP transduces signal through the release and translocation of AICD into nucleus. Intriguingly, Cao and Sudhof found that AICD interacts with Fe65 as well as Tip60 thereby regulating the transcription [9]. In support with this notion, Baek et al. [10] described that the nuclear AICD/Fe65/Tip60 complex can displace N-CoR co-repressor complex and activate the transcription of KAI1 gene. Telese et al. [11] demonstrated that the nucleosome assembly factor SET is required for the nuclear AICD/Fe65/Tip60 complex-mediated transactivation of KAI1 gene. Although these observations suggest that AICD participates in the transcriptional

* Corresponding author. Fax: +81 43 265 4459.
E-mail address: akiranak@chiba-cc.jp (A. Nakagawara).
[1] These authors contributed equally to this work.

0006-291X/$ - see front matter © 2006 Elsevier Inc. All rights reserved.
doi:10.1016/j.bbrc.2006.09.162

regulation in combination with Fe65 and Tip60, the physiological target(s) that is activated by this nuclear complex remains to be identified. As described [12–14], the activation of tumor suppressor p53 might contribute to the genesis of AD and other neurodegenerative diseases of the adult central nervous system, however, the signal(s) responsible for the activation of p53 during this process is not known. Of note, mutant form of APP derived from familial AD (FAD) enhances the p53-dependent transactivation [15,16]. In addition, Legube et al. [17] found that Tip60 associates with p53 and functions as a p53 co-activator. Thus, it is likely that there could exist a functional interaction between APP and p53. In the present study, we found that AICD interacts with p53 and enhances its transcriptional and pro-apoptotic functions, suggesting that AICD-mediated activation of p53 might be one of the cytotoxic mechanisms exerted by AICD in neuronal cells.

Materials and methods

Cell culture and transfection. U2OS and H4 cells were maintained in DMEM supplemented with 10% heat-inactivated fetal bovine serum (FBS) and antibiotic mixture. H1299 and SH-SY5Y cells were grown in RPMI-1640 supplemented with 10% heat-inactivated FBS and antibiotic mixture. Transfection was performed using LipofectAMINE 2000 (Invitrogen).

Immunofluorescence. Cells were fixed in 3.7% formaldehyde and permeabilized with 0.2% Triton X-100. Cells were then incubated with anti-FLAG antibody (M2, Sigma) followed by an incubation with FITC-conjugated secondary antibody (Invitrogen) and observed under Fluoview laser scanning confocal microscope (Olympus).

Immunoblotting. Lysates were subjected to SDS–PAGE and transferred onto Immobilon-P membranes (Millipore). Membranes were incubated with anti-p53 (DO-1, Oncogene Research Products), anti-$p21^{WAF1}$ (Ab-1, Oncogene Research Products), anti-phosphorylated from of p53 at Ser-15 (Cell Signaling), anti-APP, or anti-actin antibody (20–33, Sigma), and developed with an ECL system (Amersham Biosciences).

Immunoprecipitation. Precleared lysates were incubated with the indicated antibodies followed by incubation with protein G–Sepharose beads. Immune complexes were washed with lysis buffer, eluted in 2× SDS-sample buffer, and separated by SDS–PAGE. Gels were transferred onto Immobilon-P membranes, and immunoblotted.

Cell fractionation. Cells were lysed in lysis buffer containing 10 mM Tris–Cl, pH 7.5, 1 mM EDTA, 0.5% NP-40, and protease inhibitor cocktail. Lysates were centrifuged to separate soluble (cytoplasmic) from insoluble (nuclear) fraction. Nuclear and cytoplasmic fractions were analyzed by immunoblotting with anti-Lamin B (Ab-1, Oncogene Research Products), or anti-tubulin α antibody (Ab-2, NeoMarkers), respectively.

Cell viability assay. Cells were transferred to fresh medium containing cisplatin, incubated for 24 h, and 10 μl MTT solution was added to each well. After 1 h of incubation at 37 °C, absorbance readings for each well were performed at 570 nm using the microplate reader (Model 450, Bio-Rad).

Apoptosis assay. U2OS cells were transfected with GFP expression plasmid together with expression plasmid for APP-C57-FLAG or APP-C59-FLAG. Forty-eight hours after transfection, transfected cells were identified by the presence of green fluorescence. Cell nucleus was stained with DAPI.

Luciferase reporter assay. U2OS cells were transfected with p53-responsive luciferase reporter ($p21^{WAF1}$ or MDM2), pRL-TK *Renilla* luciferase cDNA, and p53 expression plasmid along with or without the increasing amounts of expression plasmid for APP-C57-FLAG or APP-C59-FLAG, and subjected to dual-luciferase assay (Promega).

Colony formation assay. H1299 cells were transfected with empty plasmid, p53 expression plasmid, or with p53 expression plasmid plus expression plasmid for APP-C57-FLAG or APP-C59-FLAG. Forty-eight hours after transfection, cells were transferred to the fresh medium containing G418 (400 μg/ml). After 14 days of selection, the plates were stained with Giemsa's solution.

Results

APP is associated with endogenous p53

To test whether there could exist an interaction between APP and p53 during the neuronal apoptosis, human neuroblastoma SH-SY5Y cells bearing wild-type p53 were exposed to cisplatin (CDDP). In accordance with the previous observations [18], SH-SY5Y cells underwent apoptosis in response to CDDP (data not shown). Next, we examined the protein levels of p53 and APP during the CDDP-mediated apoptosis. As shown in Fig. 1, p53 was induced in cells exposed to CDDP in association with an up-regulation of $p21^{WAF1}$ which is one of the p53-targets. In addition, a remarkable phosphorylation of p53 at Ser-15 was detected in response to CDDP. Protein levels of APP remained unchanged regardless of CDDP treatment. Of note, the immunoprecipitation of cell lysates with anti-APP antibody which recognizes the extreme COOH-terminal region of APP [19] resulted in a co-immunoprecipitation of p53 with APP. These observations suggest that APP and/or APP intracellular domain (AICD) might be associated with endogenous p53.

Interaction between AICD and p53

To examine whether AICD could interact with p53, we generated expression plasmids encoding APP-C57 and APP-C59 tagged with FLAG peptide on their

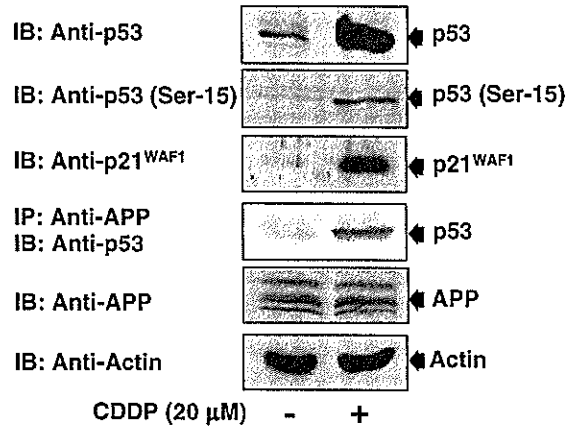

Fig. 1. Interaction between APP and endogenous p53. SH-SY5Y cells were treated with CDDP (20 μM) or left untreated. Twenty-four hours after CDDP treatment, cell lysates were subjected to immunoblotting with the indicated antibodies. Immunoblotting for actin is shown as a control for protein loading. For immunoprecipitation, equal amounts of cell lysates (1 mg of protein) were immunoprecipitated with anti-APP antibody and the immunoprecipitates were processed for immunoblotting with anti-p53 antibody.

COOH-termini (APP-C57-FLAG and APP-C59-FLAG, respectively). Human neuroglioma H4 cells were transfected with APP-C57-FLAG or APP-C59-FLAG expression plasmid and transfected cells were fixed followed by staining with anti-FLAG antibody. Consistent with the previous reports [6,8,20], APP-C57-FLAG and APP-C59-FLAG were detected both in cytoplasm and nucleus (Fig. 2A). Similar results were also obtained in immunoblotting using cytoplasmic and nuclear fractions prepared from H4 cells expressing APP-C57-FLAG or APP-C59-FLAG (Fig. 2B).

To verify the interaction between AICD and p53, cell lysates prepared from H4 cells co-transfected with expression plasmids for APP-C57-FLAG and p53 were immunoprecipitated with the normal mouse serum (NMS) or anti-p53 antibody followed by immunoblotting with anti-APP or anti-p53 antibody. As shown in Fig. 2C, APP-C57-FLAG was efficiently co-immunoprecipitated with p53. Similar to SH-SY5Y cells, H4 cells underwent apoptosis in response to CDDP in association with a significant induction of p53 (data not shown). To confirm the interaction between AICD and the endogenous p53, H4

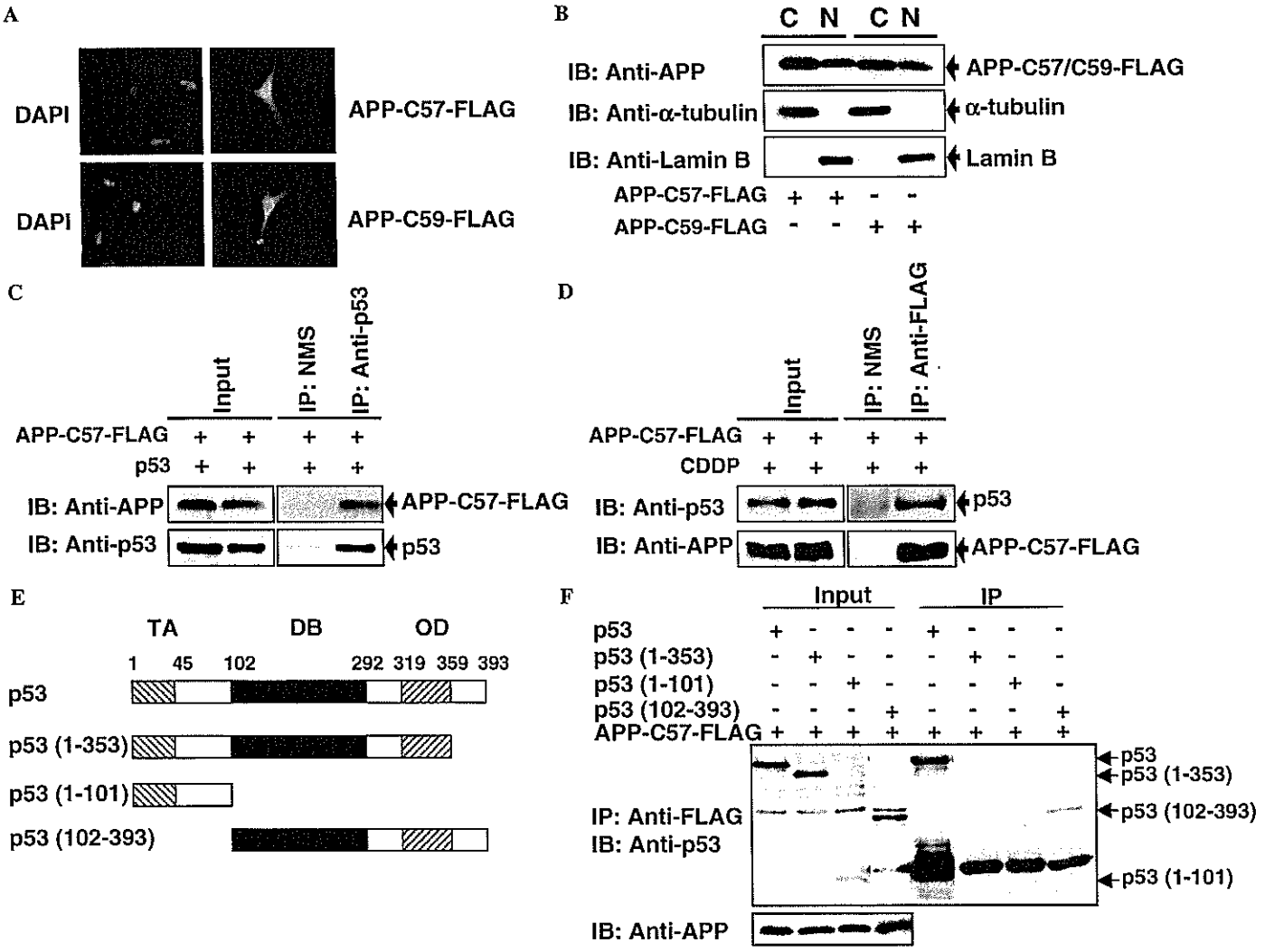

Fig. 2. Complex formation between nuclear AICD and p53 in cells. (A,B) Subcellular localization of AICD. H4 cells were transfected with the expression plasmid for APP-C57-FLAG or APP-C59-FLAG. Forty-eight hours after transfection, cells were fixed and incubated with anti-FLAG antibody. Cell nuclei were stained with DAPI (A). For subcellular fractionation, H4 cells were transfected as in (A). Transfected cells were fractionated into cytoplasmic (C) and nuclear (N) fractions. Each fraction was subjected to immunoblotting with anti-APP antibody. α-Tubulin and lamin B were used as cytoplasmic and nuclear markers, respectively. (C,D) AICD interacts with p53. H4 cells were co-transfected with expression plasmids encoding APP-C57-FLAG plus p53. Forty-eight hours after transfection, cell lysates were immunoprecipitated with normal mouse serum (NMS) or with anti-p53 antibody followed by immunoblotting with anti-APP or with anti-p53 antibody (C). For the interaction of AICD with the endogenous p53, H4 cells were transfected with the expression plasmid for APP-C57-FLAG. Twenty-four hours after transfection, cells were exposed to CDDP (20 μM) for 24 h. Cell lysates were subjected to immunoprecipitation with NMS or anti-FLAG antibody. The immunoprecipitates were analyzed by immunoblotting with anti-p53 or anti-APP antibody (D). (E,F) The COOH-terminal region of p53 is required for the interaction with AICD. H1299 cells were co-transfected with the expression plasmid for APP-C57-FLAG together with the indicated expression plasmids for p53 deletion mutants (E). Cell lysates were subjected to the immunoprecipitation with anti-APP and immunoblotted with anti-p53 antibody (F).

cells were transfected with the APP-C57-FLAG expression plasmid followed by exposure to CDDP for 24 h. As seen in Fig. 2D, the endogenous p53 was co-immunoprecipitated with APP-C57-FLAG. APP-C59-FLAG was also co-immunoprecipitated with p53 (data not shown). To identify the region(s) of p53 required for the interaction with AICD, p53-deficient H1299 cells were co-transfected with the APP-C57-FLAG expression plasmid together with the indicated expression plasmids for p53 deletion mutants (Fig. 2E). Immunoprecipitation demonstrated that APP-C57-FLAG binds to the COOH-terminal region of p53 (Fig. 2F). Thus, it is likely that nuclear AICD can interact with p53 and might modulate its function.

AICD promotes apoptosis in a p53-dependent manner

To examine whether the AICD-mediated apoptosis could be dependent on p53, H1299 cells were co-transfected with the constant amount of GFP expression plasmid together with the expression plasmid for p53, APP-C57-FLAG or APP-C59-FLAG. Forty-eight hours after transfection, transfected cells were identified by the presence of green fluorescence and the number of GFP-positive cells with apoptotic nuclei was scored. Consistent with the previous observations [21], enforced expression of p53 led to a significant induction of apoptosis (Fig. 3A). In contrast, APP-C57-FLAG and APP-C59-FLAG did not promote apoptosis. The ectopically expressed APP-C57-FLAG and APP-C59-FLAG induced apoptosis in U2OS cells (Fig. 3B). Since U2OS cells carry wild-type p53, our present results showed a good correlation between an ability of AICD to induce apoptosis and the p53 status.

AICD enhances the transcriptional and pro-apoptotic activities of p53

To address whether AICD could enhance the transcriptional activity of p53, U2OS cells were co-transfected with the constant amount of p53 expression plasmid and the luciferase reporter construct containing p53-responsive promoter derived from $p21^{WAF1}$ or MDM2 gene together with or without the increasing amounts of the expression plasmid for APP-C57-FLAG or APP-C59-FLAG. As shown in Fig. 4A, APP-C57-FLAG enhanced the p53-mediated transcriptional activity toward $p21^{WAF1}$ and MDM2 promoters in a dose-dependent manner. Similar results were also obtained in cells expressing APP-C59-FLAG (Fig. 4B).

Next, we examined a possible effect of AICD on the pro-apoptotic activity of p53. H1299 cells were transfected with the expression plasmid for p53, APP-C57-FLAG or APP-C59-FLAG. Following selection in G418, there was a drastic reduction of colony formation after transfection with p53 expression plasmid as compared with the empty plasmid, whereas APP-C57-FLAG or APP-C59-FLAG alone had undetectable effects (Fig. 4C). Intriguingly, co-expression of p53 with APP-C57-FLAG or APP-C59-FLAG reduced the colony formation as compared with p53 alone (Fig. 4D and E). Taken together, our present findings strongly suggest that AICD transduces apoptotic signals from cell surface to cell nucleus and might act as a co-activator of p53.

Discussion

AICD modulates gene transactivation in collaboration with Fe65 and Tip60 [9–11] and induces apoptosis in certain cells, which is dependent on its nuclear access [6]. Thus, it is likely that AICD has a potential role in transducing an apoptotic signal from cell surface to the nucleus, however, the detailed molecular mechanisms behind the AICD-mediated apoptotic response remain to be determined. In this study, we demonstrated that AICD interacts with p53 and enhances its transcriptional and pro-apoptotic functions. Our present findings provide a novel insight into understanding how γ-secretase cleavage of APP could lead to the neurodegeneration.

Cytosolic AICD has a short half-life and its stability is enhanced through the interaction with Fe65 [7,8]. Fe65 is an adaptor protein containing a central WW domain and two COOH-terminal phosphotyrosine-binding domains (PTB1 and PTB2) [22], and has a transactivation potential

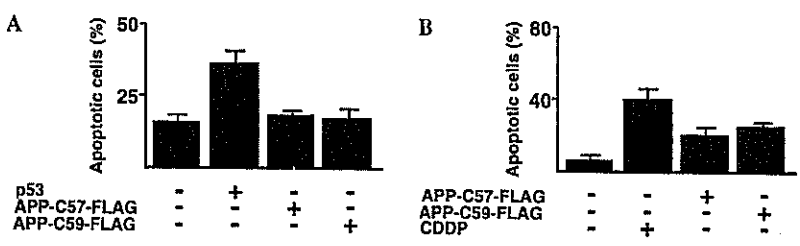

Fig. 3. AICD induces apoptosis in a p53-dependent manner. (A) AICD has undetectable effect on H1299 cells. H1299 cells were co-transfected with the constant amount of GFP expression plasmid (200 ng) together with the empty plasmid (800 ng), expression plasmid for p53 (200 ng), APP-C57-FLAG (800 ng) or APP-C59-FLAG (800 ng). Forty-eight hours after transfection, transfected cells were identified by the presence of green fluorescence. Cell nuclei were stained with DAPI to reveal nuclear condensation and fragmentation. The number of GFP-positive cells with apoptotic nuclei was scored. (B) AICD induces apoptosis in U2OS cells. U2OS cells were co-transfected with the constant amount of GFP expression plasmid (200 ng) along with the empty plasmid (800 ng), 800 ng of the expression plasmid encoding APP-C57-FLAG or APP-C59-FLAG. Twenty-four hours after transfection, cells were treated with 20 μM of CDDP for 24 h or left untreated and then the number of apoptotic cells was measured as in (A).

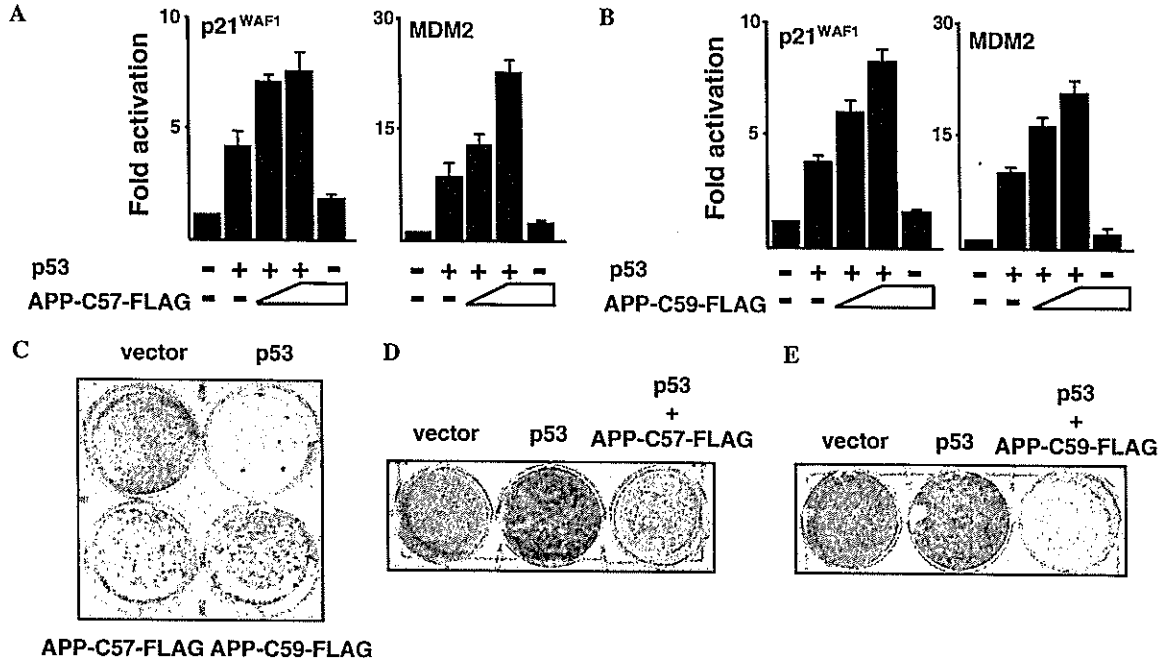

Fig. 4. AICD enhances the p53-mediated transcriptional and pro-apoptotic activities. (A,B) Luciferase reporter assay. U2OS cells were co-transfected with the constant amount of the expression plasmid for p53 (25 ng), p53-responsive luciferase reporter construct carrying the $p21^{WAF1}$ or MDM2 promoter (100 ng), *Renilla* luciferase cDNA (10 ng) together with or without the increasing amounts of the expression plasmid for APP-C57-FLAG (100 and 200 ng) (A) or APP-C59-FLAG (100 and 200 ng) (B). Forty-eight hours after transfection, cells were lysed and their luciferase activities were analyzed. Results are shown as fold-induction of the firefly luciferase activity compared with control cells. (C–E) Colony formation assay. H1299 cells were transfected with pcDNA3 (1 μg), the expression plasmid for p53 (200 ng), APP-C57-FLAG (800 ng) or APP-C59-FLAG (800 ng). Total amount of the expression plasmids was kept constant (1 μg) with pcDNA3. At 48 h post-transfection, cells were maintained in the culture medium containing G418 (400 μg/ml). After 2 weeks of selection, the plates were stained with Giemsa's solution (C). To examine the effect of APP-C57 or APP-C59 on p53, H1299 cells were transfected with the constant amount of the expression plasmid for p53 (50 ng) together with or without the expression plasmid encoding APP-C57-FLAG (400 ng) (D) or APP-C59-FLAG (400 ng) (E). Forty-eight hours after transfection, cells were kept in the medium containing G418 for 2 weeks and surviving colonies were stained as described in (C).

depending on its WW domain [23]. Tip60 with a histone acetyltransfecrase activity acts as a co-activator for AICD/Fe65 complex [9]. Tip60 alone has no transactivation function [9]. Additionally, Tip60 is part of a large nuclear protein complex, which possesses a DNA-binding activity [24]. To understand the molecular mechanisms underlying the nuclear AICD/Fe65/Tip60-mediated transcriptional regulation, it is necessary to identify nuclear protein(s) with a sequence-specific DNA-binding activity. According to our present results, AICD interacts with p53 and enhances its transcriptional activity, suggesting that p53 is one of the sequence-specific transcription factors in the nuclear AICD/Fe65/Tip60 complex. Of note, Legube et al. [17] described that Tip60 is associated with p53 and functions as a co-activator for p53. Deletion analysis revealed that AICD binds to the COOH-terminal region of p53. Since the p53 COOH-terminal region has an inhibitory effect on its DNA-binding activity, it is possible that AICD reduces its inhibitory effect.

Alternatively, Kim et al. [25] reported that AICD forms a complex with Fe65 and CP2/LSF/LBP1 family, and induces the expression of glycogen synthase kinase 3β (GSK3β). According to their results, AICD-mediated up-regulation of GSK3β led to neuronal apoptosis. Intriguingly, Watcharasit et al. [26] demonstrated that nuclear GSK3β interacts with p53 and promotes its apoptotic response. Therefore, it is possible that AICD contributes to the formation of p53/GSK3β complex, thereby enhancing the p53-mediated pro-apoptotic activity. Additionally, c-Abl binds to Fe65 and stimulates the AICD/Fe65-mediated transactivation [27]. Considering that c-Abl enhances the transcriptional activity of p53 [28], it is likely that c-Abl might be involved in the AICD-dependent activation of p53.

Recently, Esposito et al. [16] reported that the inhibition of β-secretase cleavage of FAD-linked APP mutant significantly reduces the p53-mediated transcriptional activation. They also described that the treatment of FAD-associated APP mutant-expressing cells with γ-secretase inhibitor can confer resistance to apoptotic stimuli. APP missense mutations found in FAD led to an increased production of Aβ42, which might be due to the increased cleavage of APP by γ-secretase [29]. The accumulation of Aβ42 caused the neuronal apoptosis and this process was mediated through the activation of p53/Bax cell death pathway [30], suggesting that there could exist a functional interaction between intracellular Aβ42 and proximal effector(s) of this pathway. However, the precise molecular mechanisms by which p53 is activated by intracellular Aβ42 remain to be clarified. During the preparation of our

manuscript, Alves da Costa et al. [31] described that AICD enhances the transcriptional activity of p53 through the up-regulation of p53 at mRNA level. Under our experimental conditions, AICD had negligible effects on the mRNA level of p53 as examined by RT-PCR (data not shown). It might be due to the different cell systems. Collectively, it is likely that the intracellular Aβ and/or nuclear AICD might induce neuronal apoptosis at least in part through the activation of the p53-dependent pro-apoptotic pathway.

Acknowledgments

This work was supported in part by a Grant-in-Aid from the Ministry of Health, Labour and Welfare for Third Term Comprehensive Control Research for Cancer, a Grant-in-Aid for Scientific Research on Priority Areas from the Ministry of Education, Culture, Sports, Science and Technology, Japan, and a Grant-in-Aid for Scientific Research from Japan Society for the Promotion of Science.

References

[1] J. Kang, H.G. Lemaire, A. Unterbeck, J.M. Salbaum, C.L. Masters, K.H. Grzeschik, G. Multhaup, K. Beyreuther, B. Muller-Hill, The precursor of Alzheimer's disease amyloid A4 protein resembles a cell-surface receptor, Nature 325 (1987) 733–736.

[2] S.F. Lichtenthaler, C. Haass, Amyloid at the cutting edge: activation of alpha-secretase prevents amyloidogenesis in an Alzheimer disease mouse model, J. Clin. Invest. 113 (2004) 1384–1387.

[3] D.J. Selkoe, Alzheimer's disease: genes, proteins, and therapy, Physiol. Rev. 81 (2001) 741–766.

[4] C.J. Pike, D. Burdick, A.J. Walencewicz, C.G. Glabe, C.W. Cotman, Neurodegeneration induced by beta-amyloid peptides in vitro: the role of peptide assembly state, J. Neurosci. 13 (1993) 1676–1687.

[5] B. Passer, L. Pellegrini, C. Russo, R.M. Siegel, M.J. Lenardo, G. Schettini, M. Bachmann, M. Tabaton, L. D'Adamio, Generation of an apoptotic intracellular peptide by gamma-secretase cleavage of Alzheimer's amyloid beta protein precursor, J. Alzheimers Dis. 2 (2000) 289–301.

[6] A. Kinoshita, C.M. Whelan, O. Berezovska, B.T. Hyman, Neurodegeneration induced by beta-amyloid peptides in vitro: the role of peptide assembly state, J. Biol. Chem. 277 (2002) 28530–28536.

[7] P. Cupers, I. Orlans, K. Craessaerts, W. Annaert, B. De Strooper, The amyloid precursor protein (APP)-cytoplasmic fragment generated by gamma-secretase is rapidly degraded but distributes partially in a nuclear fraction of neurones in culture, J. Neurochem. 78 (2001) 1168–1178.

[8] W.T. Kimberly, J.B. Zheng, S.Y. Guenette, D.J. Selkoe, The intracellular domain of the beta-amyloid precursor protein is stabilized by Fe65 and translocates to the nucleus in a notch-like manner, J. Biol. Chem. 276 (2001) 40288–40292.

[9] X. Cao, T.C. Sudhof, A transcriptionally correction of trascriptively active complex of APP with Fe65 and histone acetyltransferase Tip60, Science 293 (2001) 115–120.

[10] S.H. Baek, K.A. Ohgi, D.W. Rose, E.H. Koo, C.K. Glass, M.G. Rosenfeld, Exchange of N-CoR corepressor and Tip60 coactivator complexes links gene expression by NF-kappaB and beta-amyloid precursor protein, Cell 110 (2002) 5–67.

[11] F. Telese, P. Bruni, A. Donizetti, D. Gianni, C. D'Ambrosio, A. Scaloni, N. Zambrano, M.G. Rosenfield, T. Russo, Transcription regulation by the adaptor protein Fe65 and the nucleosome assembly factor SET, EMBO Rep. 6 (2005).77–82.

[12] R.S. Slack, D.J. Belliveau, M. Rosenberg, J. Atwal, H. Lochmuller, R. Aloyz, A. Haghighi, B. Lach, P. Seth, E. Cooper, F.D. Miller, Adenovirus-mediated gene transfer of the tumor suppressor, p53, induces apoptosis in postmitotic neurons, J. Cell Biol. 135 (1996) 1085–1096.

[13] H. Xiang, D.W. Hochman, H. Saya, T. Fujiwara, P.A. Schwartzkroin, R.S. Morrison, Evidence for p53-mediated modulation of neuronal viability, J. Neurosci. 16 (1996) 6753–6765.

[14] P.E. Hughes, T. Alexi, M. Dragunow, A role for the tumour suppressor gene p53 in regulating neuronal apoptosis, Neuroreport 8 (1997) v–xii.

[15] X. Xu, D. Yang, T. Wyss-Coray, J. Yan, L. Gan, Y. Sun, L. Mucke, Wild-type but not Alzheimer-mutant amyloid precursor protein confers resistance against p53-mediated apoptosis, Proc. Natl. Acad. Sci. USA 96 (1999) 7547–7552.

[16] L. Esposito, L. Gan, G.Q. Yu, C. Essrich, L. Mucke, Intracellularly generated amyloid-beta peptide counteracts the antiapoptotic function of its precursor protein and primes proapoptotic pathways for activation by other insults in neuroblastoma cells, J. Neurochem. 91 (2004) 1260–1274.

[17] G. Legube, L.K. Linares, S. Tyteca, C. Caron, M. Scheffner, M. Chevillard-Briet, D. Trouche, Role of the histone acetyl transferase Tip60 in the p53 pathway, J. Biol. Chem. 279 (2004) 44825–44833.

[18] T. Nakagawa, M. Takahashi, T. Ozaki, K. Watanabe, S. Todo, H. Mizuguchi, T. Hayakawa, A. Nakagawara, Autoinhibitory regulation of p73 by Delta Np73 to modulate cell survival and death through a p73-specific target element within the Delta Np73 promoter, Mol. Cell. Biol. 22 (2002) 2575–2585.

[19] K. Takio, M. Hasegawa, K. Titani, Y. Ihara, Identification of beta protein precursor in newborn rat brain, Biophys. Biochem. Res. Commun. 160 (1989) 1296–1301.

[20] Y. Gao, S.W. Pimplinkar, The gamma -secretase-cleaved C-terminal fragment of amyloid precursor protein mediates signaling to the nucleus, Proc. Natl. Acad. Sci. USA 98 (2001) 14979–14984.

[21] C.J. Di Como, C. Gaiddon, C. Prives, p73 function is inhibited by tumor-derived p53 mutants in mammalian cells, Mol. Cell. Biol. 19 (1999) 1438–1449.

[22] J.P. Borg, J. Ooi, E. Levy, B. Margolis, The phosphotyrosine interaction domains of X11 and FE65 bind to distinct sites on the YENPTY motif of amyloid precursor protein, Mol. Cell. Biol. 16 (1996) 6229–6241.

[23] X. Cao, T.C. Sudhof, Dissection of amyloid-beta precursor protein-dependent transcriptional transactivation, J. Biol. Chem. 279 (2004) 24601–24611.

[24] T. Ikura, V.V. Ogryzko, M. Grigoriev, R. Groisman, J. Wang, M. Horikoshi, R. Scully, J. Qin, Y. Nakatani, Involvement of the TIP60 histone acetylase complex in DNA repair and apoptosis, Cell 102 (2002) 463–473.

[25] H.S. Kim, E.M. Kim, J.P. Lee, C.H. Park, S. Kim, J.H. Seo, K.A. Chang, E. Yu, S.J. Jeong, Y.H. Chong, Y.H. Suh, C-terminal fragments of amyloid precursor protein exert neurotoxicity by inducing glycogen synthase kinase-3 beta expression, FASEB J. 17 (2003) 1951–1953.

[26] P. Watcharasit, G.N. Bijur, J.W. Zmijewski, L. Song, A. Zmijewska, X. Chen, G.V.W. Johnson, R.S. Jope, Glycogen synthase kinase-3beta (GSK3beta) binds to and promotes the actions of p53, Proc. Natl. Acad. Sci. USA 99 (2002) 7951–7955.

[27] M.S. Perkinton, C.L. Standen, K.F. Lau, S. Kesavapany, H.L. Byers, M. Ward, D.M. McLoughlin, C.C.J. Miller, The c-Abl tyrosine kinase phosphorylates the Fe65 adaptor protein to stimulate Fe65/amyloid precursor protein nuclear signaling, J. Biol. Chem. 279 (2004) 22084–22091.